

Synthesis, Structure, Ligand Dynamics, and Catalytic Activity of Cationic $[\text{Pd}(\eta^3\text{-allyl})(\kappa^2(E,N)\text{-EN-chelate})]^+$ ($E = \text{P}, \text{O}, \text{S}, \text{Se}$) Complexes

Bernhard Bichler,[†] Luis F. Veiros,^{||} Özgür Öztopcu,[†] Michael Puchberger,[‡] Kurt Mereiter,[§] Kouki Matsubara,^{#,⊥} and Karl A. Kirchner^{*,†}

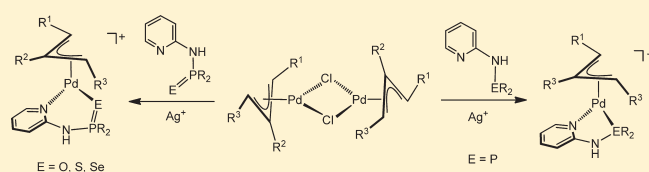
[†]Institute of Applied Synthetic Chemistry, [‡]Institute of Materials Chemistry, and [§]Institute of Chemical Technologies and Analytics, Vienna University of Technology, Getreidemarkt 9, A-1060 Vienna, Austria

[#]Department of Chemistry, Faculty of Science, Fukuoka University, 8-19-1 Nanakuma, Fukuoka 814-0180, Japan

^{||}Centro de Química Estrutural, Instituto Superior Técnico, Universidade Técnica de Lisboa, 1049-001 Lisboa, Portugal

S Supporting Information

ABSTRACT: A series of cationic palladium allyl complexes of the type $[\text{Pd}(\eta^3\text{-allyl})(\kappa^2(E,N)\text{-EN-chelate})]^+$ containing several heterodifunctional EN ($E = \text{P}, \text{O}, \text{S}, \text{Se}$) ligands based on *N*-(2-pyridinyl)aminophosphines and oxo, thio, and seleno derivatives thereof are prepared. These complexes are studied by one- and two-dimensional NMR techniques together with X-ray and DFT calculations. Variable-temperature and phase-sensitive ^1H , ^1H NOESY NMR measurements reveal both allyl and EN ligand dynamics. In the case of palladium, PN complexes' η^3 to η^1 isomerization takes place by opening the η^3 -allyl group selectively at the *trans* position with respect to the phosphorus center, while for EN ($E = \text{O}, \text{S}, \text{Se}$) complexes an "apparent" allyl rotation is observed preceding with Pd–E and Pd–N bond breaking. DFT calculations indicate that both isomerization processes are solvent assisted, in agreement with the NMR data. In addition, the use of the new palladium allyl complexes has been examined as catalysts for Suzuki–Miyaura coupling of various aryl bromides and arylboronic acids. $[\text{Pd}(\eta^3\text{-CHPhCHCH}_2)(\text{ON-Ph})]^+$, bearing an η^3 -cinnamyl ligand, is one of the most efficient catalysts, converting aryl bromides and arylboronic acids at 80 °C with a catalyst loading of 0.1 mol % quantitatively into the expected biaryl products.

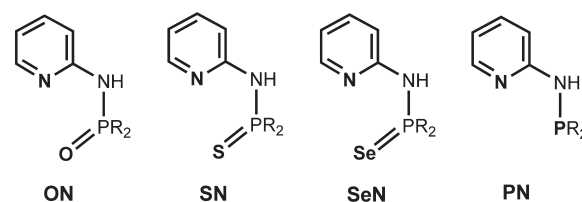


INTRODUCTION

Heterodifunctional ligands are intensively studied and applied in coordination and organometallic chemistry owing to the often unique properties of their metal complexes and their ability to generate hemilabile systems, which often display enhanced reactivity.¹ In particular soft/hard, e.g., P/N and P/O, assemblies are able to coordinate reversibly to a metal center, providing or protecting temporarily a vacant coordination site, a feature very desirable for catalysts.

In this context, we have become interested in heterodifunctional PN ligands based on 2-aminopyridine in which the pyridine moiety is separated by an amino group.^{2,3} Due to the comparative ease of phosphorus–nitrogen bond forming reactions compared to phosphorus–carbon bonds, it is not surprising that many examples of transition metal complexes featuring this type of PN ligands have emerged over the last decades.^{4–13} The most prominent member of these ligand family, with a few exceptions,¹⁴ is *N*-diphenylphosphino-2-aminopyridine (PN-Ph). Another very useful and interesting aspect of PN ligands is the fact that they can be readily functionalized also at the phosphorus site by oxidation with H_2O_2 , sulfur, and gray selenium, respectively, to give chalcogen O, S, and Se derivatives (EN ligands). Despite the fact that the synthesis of these heterodifunctional EN ligands has been known for some time,¹⁰ it is surprising that transition metal complexes containing these ligands are relatively scarce.^{6,9,15,16}

Chart 1

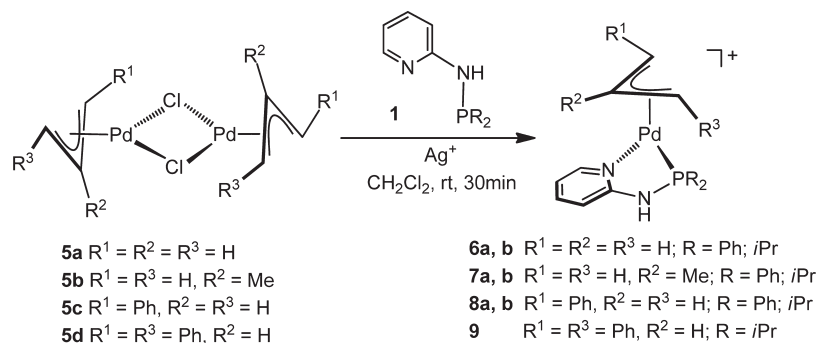


As part of our ongoing interest in transition metal complexes containing heterodifunctional ligands,^{2,3} we herein report on the synthesis, solution and solid-state structure, and reactivity of palladium allyl complexes featuring bidentate heterodifunctional EN ($E = \text{P}, \text{O}, \text{S}, \text{Se}$) ligands with $R = \text{Ph}$ and *i*Pr as shown in Chart 1. The chemistry of palladium allyl complexes is a topic of considerable contemporary interest in view of the various fluxional processes observed in these systems and also from the point of view of the potential applications of these types of complexes in homogeneous catalysis.¹⁷

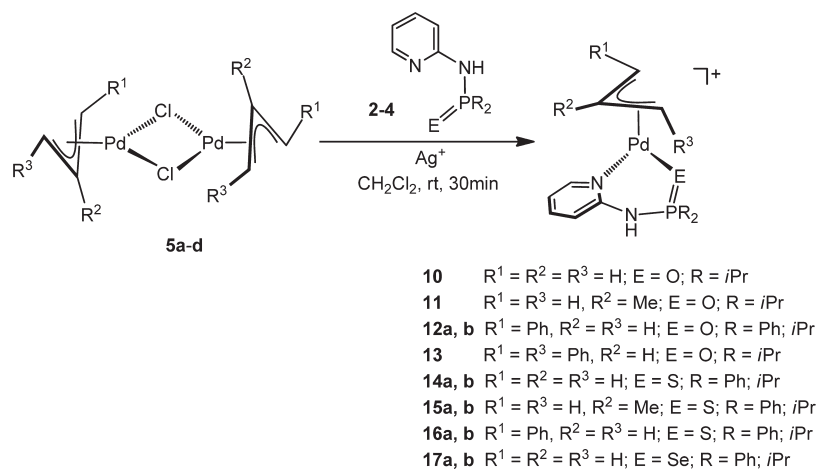
Received: August 17, 2011

Published: October 14, 2011

Scheme 1



Scheme 2

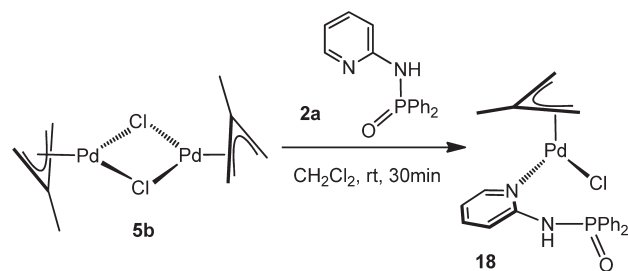


RESULTS AND DISCUSSION

Synthesis of Palladium Allyl Complexes. The cationic allyl palladium complexes $[Pd(\eta^3\text{-allyl})(\kappa^2(E,N)\text{-EN-chelate})]^+$ (**6–17**) were prepared in high yields from the reaction of the chloro-bridged palladium allyl dimers $[Pd(\eta^3\text{-allyl})(\mu\text{-Cl})_2]$ (**5a–d**) with the corresponding EN ligands PN-Ph (**1a**), PN-*i*Pr (**1b**), ON-Ph (**2a**), ON-*i*Pr (**2b**), SN-Ph (**3a**), SN-*i*Pr (**3b**), SeN-Ph (**4a**), and SeN-*i*Pr (**4b**) in the presence of $AgSbF_6$ (or $AgCF_3SO_3$) in dichloromethane (Schemes 1 and 2). If the same reaction is performed in the absence of a halide scavenger, only the strong chelating PN, SN, and SeN ligands afforded the same complexes (with chloride as counterion), whereas the weaker ON ligands gave complexes where the ligand is coordinated in $\kappa^1(N)$ -fashion. This was exemplarily shown for the reaction of $[Pd(\eta^3\text{-CH}_2\text{-CMeCH}_2)(\mu\text{-Cl})_2]$ (**5b**) with the ligand ON-Ph (**2a**), yielding the neutral complex $[Pd(\eta^3\text{-CH}_2\text{-CMeCH}_2)(\kappa^1(N)\text{-ON-Ph})Cl]$ (**18**), as shown in Scheme 3. There was no evidence for the formation of complexes of the type $[Pd(\eta^1\text{-allyl})(\kappa^2(E,N)\text{-EN})Cl]$ bearing an η^1 -coordinated allyl ligand as erroneously stated recently.¹⁸

As shown for several complexes bearing EN ligands,³ deprotonation of their acidic NH protons is typically achieved under mild conditions, leading to complexes with anionic EN^H ligands. Accordingly, as a representative example, deprotonation of the

Scheme 3



SN-*i*Pr ligand was accomplished by reacting **14b** with 1 equiv of $KOtBu$ in THF for 30 min, affording the neutral complex $[Pd(\eta^3\text{-CH}_2\text{CHCH}_2)(SN^H\text{-}iPr)]$ (**19**) in essentially quantitative yield (Scheme 4).

All allyl complexes are thermally robust pale yellow solids that are air stable both in the solid state and in solution for several days. Characterization was accomplished by elemental analysis and 1H , $^{13}C\{^1H\}$, and $^{31}P\{^1H\}$ NMR spectroscopy. In addition, the solid-state structures of representative compounds were determined by X-ray diffraction.

X-ray Diffraction Studies. The solid-state structures of the palladium allyl complexes **7b**, **8b**, **9**, **10**, **14b**, **15a**, **15b**, **17b**, **18** (as the solvate $18 \cdot 1/2CH_2Cl_2$), and **19** were determined by

Scheme 4

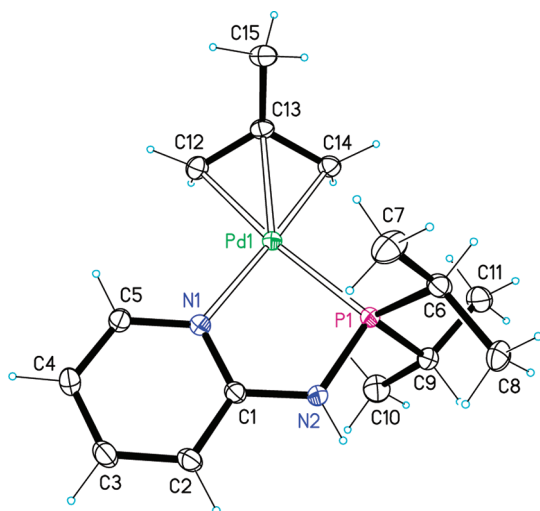
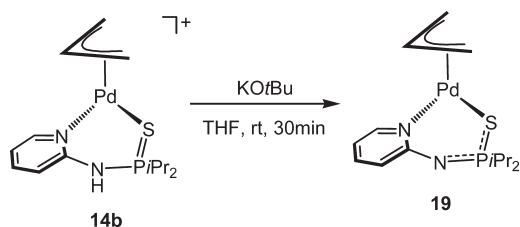


Figure 1. Molecular structure of $[\text{Pd}(\eta^3\text{-CH}_2\text{CMeCH}_2)(\text{PN-}i\text{Pr})]\text{SbF}_6$ (**7b**) showing 50% displacement ellipsoids (SbF_6^- anion omitted for clarity).

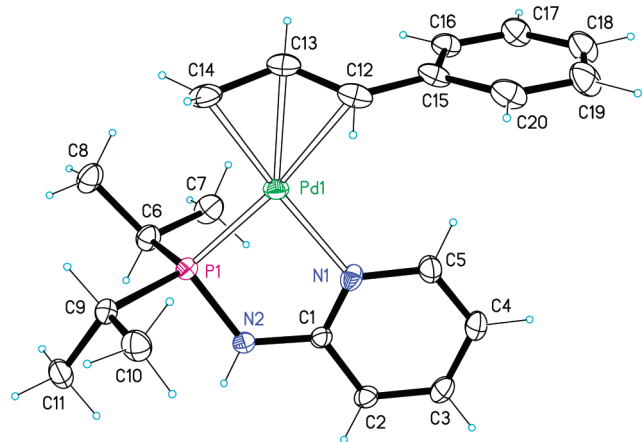


Figure 2. Molecular structure of $[\text{Pd}(\eta^3\text{-CHPhCHCH}_2)(\text{PN-}i\text{Pr})]\text{SbF}_6$ (**8b**) showing 50% displacement ellipsoids (SbF_6^- anion omitted for clarity).

single-crystal X-ray diffraction. The molecular structures of these compounds are shown in Figures 1–10. Selected bond lengths and angles and crystallographic data are provided in the Supporting Information (Tables S1 and S2). Disregarding the central allyl carbon atom C_B , the palladium coordination of all complexes can be described as square planar with the pyridine nitrogen N1, the donor atom E (P, O, S, Se, or Cl), and the allyl

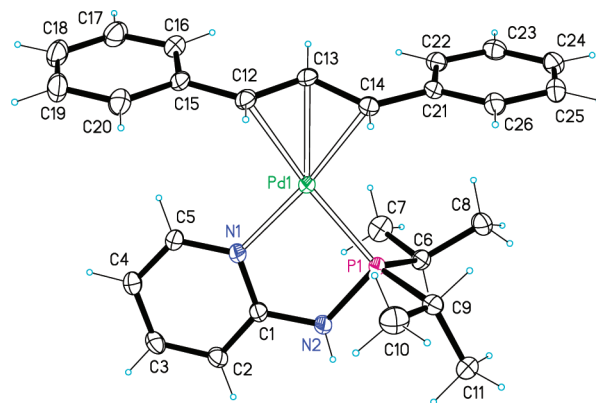


Figure 3. Molecular structure of $[\text{Pd}(\eta^3\text{-CHPhCHCHPh})(\text{PN-}i\text{Pr})]\text{SbF}_6$ (**9**) showing 50% displacement ellipsoids (SbF_6^- anion omitted for clarity).

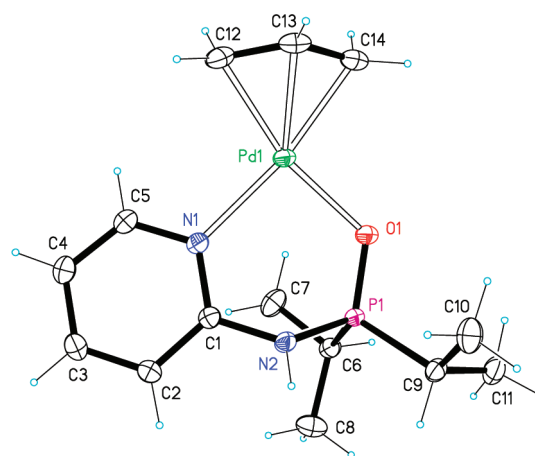


Figure 4. Molecular structure of $[\text{Pd}(\eta^3\text{-CH}_2\text{CHCH}_2)(\text{ON-}i\text{Pr})]\text{SbF}_6$ (**10**) showing 50% displacement ellipsoids (SbF_6^- anion omitted for clarity). The allyl group is orientation disordered with $C_B \equiv C13$ alternatively in one of two positions, of which only the major position is shown.

carbon atoms C_A (*cis* to N1) and C_C (*cis* to E) as the ligands. As can be seen from Table S1, the bond lengths Pd–N1, mean value 2.127 Å, and Pd– C_C (*trans* to N1), mean value 2.116 Å, are relatively uniform throughout the 10 compounds. In contrast, the bond length Pd–E varies from 2.12 to 2.48 Å and Pd– C_A varies from 2.10 to 2.28 Å.

The three pyridyl aminophosphine complexes **7b**, **8b**, and **9** contain ligands that form a largely planar five-membered chelate ring with N1–Pd1–P1 bond angles near 83°. The coordination figure about Pd, defined by the four ligand atoms N1, P1, C_A , and C_C is essentially coplanar, with the pyridine ring showing interplanar angles of only about 10°. The bond distances Pd–N, Pd–P, Pd– C_A , and Pd– C_C are each quite uniform and average 2.121, 2.259, 2.255, and 2.118 Å. This means that the Pd– C_A bonds *trans* to Pd–P are all significantly elongated compared with the Pd– C_C bonds *trans* to Pd–N. This feature is either due to bonding properties of the phosphorus ligand atoms and/or due to the low N–Pd– C_A bond angles, but it is practically independent of the substitution pattern of the allyl ligands (2-methyl, 1-phenyl, and 1,3-diphenyl).

The complexes **10**, **14b**, **15a**, **15b**, **17b**, and **19** contain six-membered chelate rings that are distinctly bent, depending on

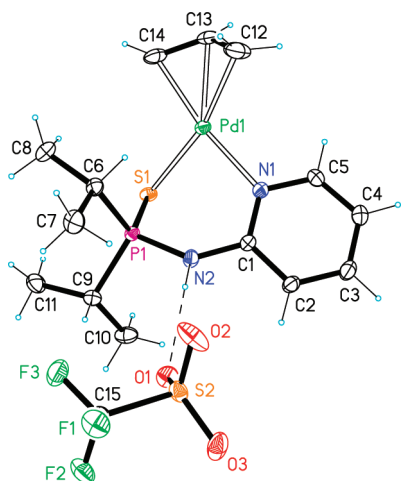


Figure 5. Molecular structure of $[\text{Pd}(\eta^3\text{-CH}_2\text{CHCH}_2)(\text{SN-}i\text{Pr})]\text{CF}_3\text{SO}_3$ (**14b**) showing 50% displacement ellipsoids. Hydrogen bond $\text{N2-H}\cdots\text{O1}$ has $\text{N2}\cdots\text{O1} = 2.920 \text{ \AA}$. The allyl group is orientation disordered with $\text{C}_B \equiv \text{C13}$ alternatively in one of two positions, of which only the major position is shown.

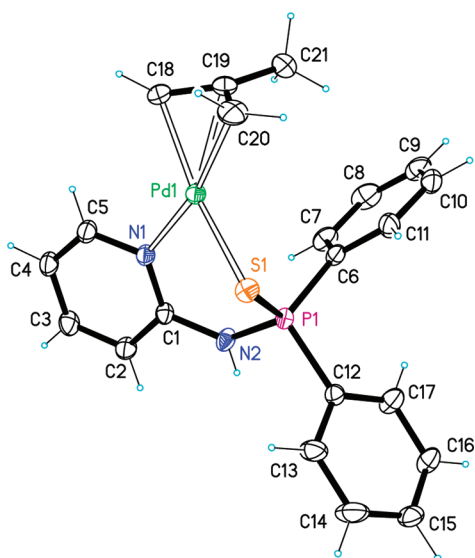


Figure 6. Molecular structure of $[\text{Pd}(\eta^3\text{-CH}_2\text{CMeCH}_2)(\text{SN-Ph})]\text{SbF}_6$ (**15a**) showing 50% displacement ellipsoids (SbF_6^- anion omitted for clarity).

the size of the additional heteroatom O, S, or Se. Hence, the angle between the pyridine ring and the plane of the four Pd ligand atoms increases from 27.7° in **10** ($\text{E} = \text{O}$) to 47.5° in **14b** ($\text{E} = \text{S}$) and finally to 49.0° in **17b** ($\text{E} = \text{Se}$). In compounds **15a** and **19** this interplanar angle is notably smaller, most likely because of the space requirement of the two P-bonded phenyl rings in **15a** and a different hybridization of the chelate ring in **19** due to the deprotonated nitrogen atom N2 (Figure 10).

The complexes **10**, **14b**, **17b**, and **19**, with unsubstituted allyl groups, show the usual static orientation disorder/order of this group whereby the allyl carbon C_B points out from the $\text{N1-E-C}_A\text{-C}_C$ coordination plane to both sides in different proportions, which vary from 0.82/0.18 for **10** to 0.57/0.43 in **19**. In the four complexes this orientation disorder practically does

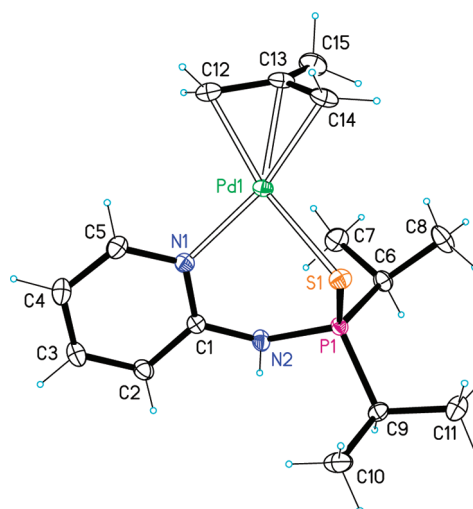


Figure 7. Molecular structure of $[\text{Pd}(\eta^3\text{-CH}_2\text{CMeCH}_2)(\text{SN-}i\text{Pr})]\text{SbF}_6$ (**15b**) showing 50% displacement ellipsoids (SbF_6^- anion omitted for clarity).

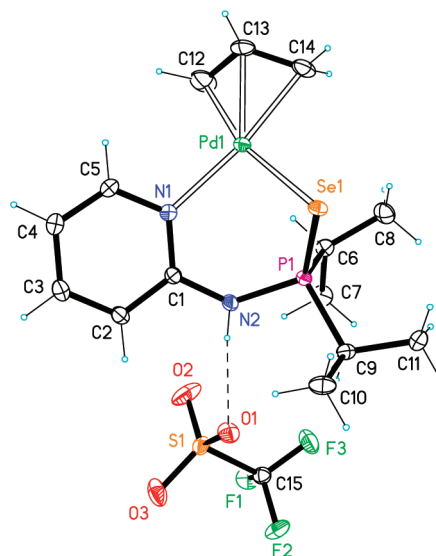


Figure 8. Molecular structure of $[\text{Pd}(\eta^3\text{-CH}_2\text{CHCH}_2)(\text{SeN-}i\text{Pr})]\text{CF}_3\text{SO}_3$ (**17b**) showing 50% displacement ellipsoids. Hydrogen bond $\text{N2-H}\cdots\text{O1}$ has $\text{N2}\cdots\text{O1} = 2.917 \text{ \AA}$. The allyl group is orientation disordered with $\text{C}_B \equiv \text{C13}$ alternatively in one of two positions, of which only the major position is shown.

not affect the positions of the C_A and C_C atoms. In contrast, the remaining six complexes with substituted allyl groups (2-methyl, 1-phenyl, and 1,3-diphenyl) show only a single allyl orientation in the solid state.

The N-H groups of the EN ligands are distinctly acidic and form therefore hydrogen bonds with available acceptor atoms. In the SbF_6 salts these are relatively straight $\text{N-H}\cdots\text{F}$ bonds with $\text{N}\cdots\text{F}$ distances between 2.84 and 3.03 \AA (**8b** is an exception because of a bifurcated bond), and in the two triflate salts the $\text{N-H}\cdots\text{O}$ bonds have $\text{N}\cdots\text{O} = 2.92 \text{ \AA}$. In the two independent complexes $[\text{Pd}(\eta^3\text{-CH}_2\text{CMeCH}_2)(\kappa^1(\text{N})\text{-ON-Ph})\text{Cl}]$ of **18** intramolecular $\text{N-H}\cdots\text{Cl}$ bonds ($\text{N}\cdots\text{Cl} = 3.19$ and 3.21 \AA) are formed instead. This propensity of the NH group for H-bond formation was also observed for the bare ligands EN with $\text{E} = \text{S}$

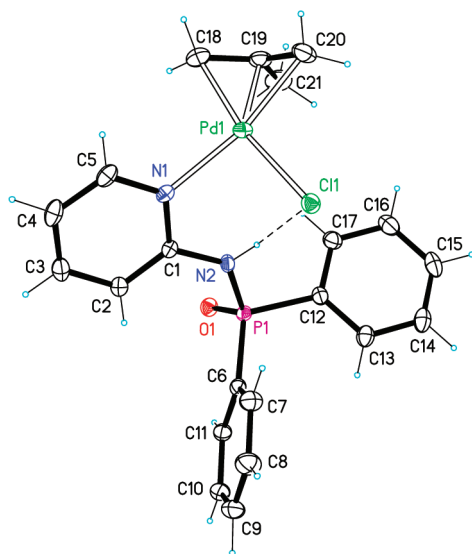


Figure 9. Molecular structure of $[\text{Pd}(\eta^3\text{-CH}_2\text{CMeCH}_2)(\kappa^1(\text{N})\text{-ON-Ph})\text{Cl}] \cdot 1/2\text{CH}_2\text{Cl}_2$ (**18** · $1/2\text{CH}_2\text{Cl}_2$) showing 50% displacement ellipsoids and only one of the two independent Pd complexes.

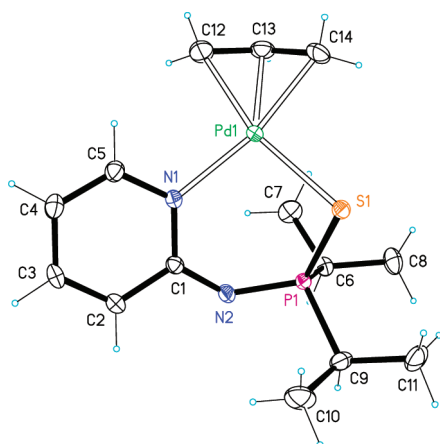


Figure 10. Molecular structure of $[\text{Pd}(\eta^3\text{-CH}_2\text{CHCH}_2)(\text{SN}^{\text{H}}\text{-iPr})]$ (**19**) with 50% displacement ellipsoids. The allyl group is orientation disordered with $\text{C}_B \equiv \text{C13}$ alternatively in one of two positions, of which only the major position is shown.

and Se, where the phenyl-substituted phosphines showed $\text{N-H} \cdots \text{N}_{\text{pyridine}}$ and the isopropyl-substituted phosphines showed $\text{N-H} \cdots \text{E}$ hydrogen bonds.³⁸ In the solid-state structures of the bare ligands **2a** and **2b**, EN with $\text{E} = \text{O}$, both phenyl- and isopropyl-substituted phosphines show $\text{N-H} \cdots \text{O}$ bonds with $\text{N} \cdots \text{O} = 2.77\text{--}2.82 \text{ \AA}$, whereas the pyridine nitrogen is inactive as an acceptor (see Supporting Information).

NMR Studies. An analysis of the $^{13}\text{C}\{^1\text{H}\}$ NMR spectra of allyl carbons of the palladium PN complexes **6–9** clearly shows P,N-coordination. A doublet is observed for each of the two terminal allyl carbon nuclei. The resonances of the terminal allyl carbon atoms *trans* to the coordinated phosphorus center appear in the range about 79 to 100 ppm with a coupling constant $^2J_{\text{P-C}}$ of 24–33 Hz, which lies in a region usually observed for *trans* $^{31}\text{P}\text{--}^{13}\text{C}$ coupling. The signal for the terminal allyl carbon nucleus *trans* to nitrogen resonates in a more shielded region (ca. 44–68 ppm) with a coupling constant $^2J_{\text{P-C}}$ on the order of

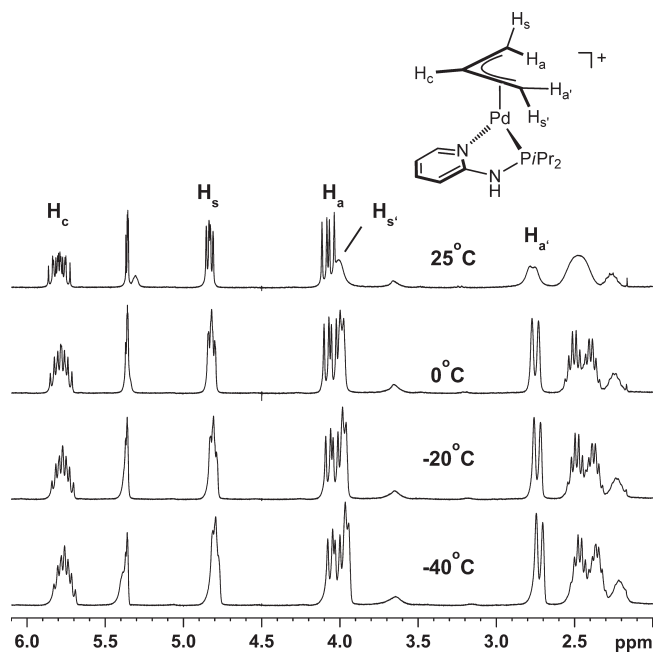


Figure 11. 300 MHz ^1H NMR variable-temperature spectra of $[\text{Pd}(\eta^3\text{-CH}_2\text{CHCH}_2)(\kappa^2(\text{P,N})\text{-PN-iPr})]\text{SbF}_6$ (**6b**) in CD_2Cl_2 from -40 to $25 \text{ }^\circ\text{C}$.

3–6 Hz, which is typical for a two-bond *cis* coupling of phosphorus and carbon nuclei. The central allyl carbon atoms give rise to doublets in the range 121 to 138 ppm, as expected for $\kappa^2(\text{P,N})$ -coordination. In the case of palladium EN ($\text{E} = \text{O}, \text{S}, \text{Se}$) complexes **10–19** all allyl carbon atoms give rise to singlet resonances at 61–90, 56–74, and 119–135 ppm, assignable to the two terminal and the central allyl carbon atoms, respectively.

In the $^{31}\text{P}\{^1\text{H}\}$ NMR spectra, the palladium PN and ON complexes **6–13** exhibit singlets that show the expected low-field shifts of the $\kappa^2(\text{P,N})$ -coordinated PN ligands relative to the free uncoordinated ligands. This trend is reversed in the case of the palladium SN and SeN complexes **14–17**. In the case of the SeN complexes **17a** and **17b**, the phosphorus signals exhibit a pair of Se satellites with $^{31}\text{P}\text{--}^{77}\text{Se}$ coupling constants of 651 and 635 Hz, respectively. The deprotonated complex **19** also displays a sharp single $^{31}\text{P}\{^1\text{H}\}$ NMR resonance at 64.2 ppm, which is significantly shifted to higher field than the starting material **14b** (cf. 100.0 ppm). The ^1H spectrum of **19** is very similar to that of **14b** except that the NH resonance is now absent.

The room-temperature ^1H NMR spectra of the PN complexes **6–9** in CD_2Cl_2 exhibit sharp signals for all protons except for the *syn* and *anti* protons H_s and H_a . These are in pseudo-*trans* position to the pyridine moiety and show slightly broadened resonances. Figure 11 shows a variable-temperature NMR study for **6b**. Lowering the temperature causes the two broad lines observed at ambient temperature to sharpen. Moreover, this exchange process is facilitated in more strongly coordinating solvents such as CD_3CN , indicating a selective dynamic η^3 to η^1 isomerization process induced by solvent coordination (*vide infra*).

The ^1H NMR spectra of the palladium EN complexes **10–17** give rise to sharp signals at room temperature but are strongly solvent (and counterion) dependent. In Figure 12, the ^1H NMR spectra of **14b** (with the poorly coordinating SbF_6^- anion) recorded in CD_2Cl_2 and CD_3CN are depicted. While in the poorly coordinating solvent CD_2Cl_2 the expected five allyl resonances

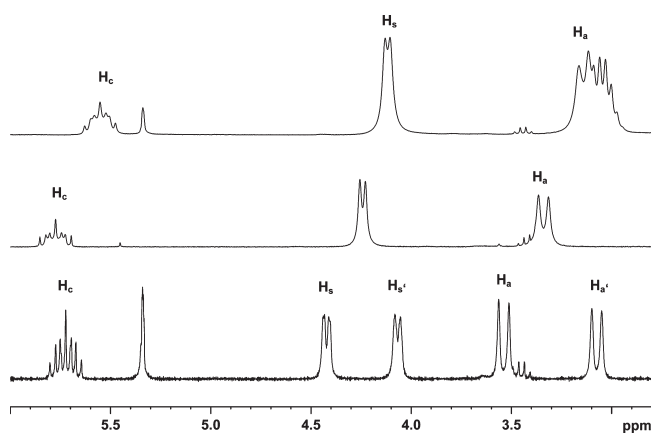
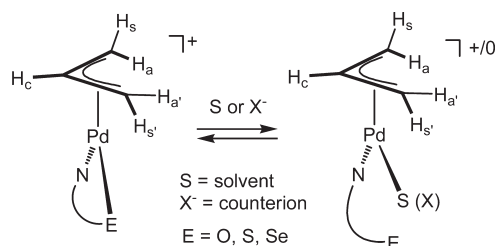


Figure 12. Section of the 300 MHz ^1H NMR spectra of $[\text{Pd}(\eta^3\text{-CH}_2\text{CHCH}_2)(\kappa^2(\text{S},\text{N})\text{-SN-}i\text{Pr})]\text{SbF}_6^-$ (**14b**) in CD_2Cl_2 (lower spectrum), in CD_3CN (middle spectrum), and in the presence of NEt_4Cl (2 equiv) in CD_2Cl_2 (upper spectrum) at 25°C .

Scheme 5



are observed, in the coordinating solvent CD_3CN the spectrum simplifies, and only three allyl resonances are observed. This observation points to a (solvent-induced) dynamic process involving the EN ligand; that is, the EN ligand is *hemilabile*, exhibiting rapid and reversible Pd–E bond cleavage and solvent coordination as indicated in Scheme 5 (*vide infra*). Noteworthy, a similar ^1H NMR spectrum is observed for **14b** with chloride as counterion dissolved in CD_2Cl_2 or when NEt_4Cl was added to **14b** (as SbF_6^- salt). In these cases, the chloride anion reversibly coordinates to the palladium center, competing with E-donor coordination (Scheme 5).

Allyl Dynamics. Palladium allyl complexes are well known^{19–27} to exhibit various dynamic processes including η^3 to η^1 isomerization and “apparent” allyl rotation. According to the literature, these allyl isomerization processes may occur via different mechanisms and may be under either electronic or steric control. In addition, these dynamics may be associated with Pd–ligand bond breaking and may be solvent or counterion assisted. In order to determine the solution structure of our palladium PN and EN complexes as well as to establish the nature of their dynamic behavior, complexes **6b** and **14b** were studied by two-dimensional NMR and DFT calculations.

a. Selective Allyl η^3 – η^1 – η^3 Isomerization. Figure 13 shows a phase-sensitive 300 MHz ^1H , ^1H NOESY for **6b** in CD_2Cl_2 at 25°C . The spectrum shows exchange peaks (black) for the *syn/anti* protons $\text{H}_{\text{S}'}$ and $\text{H}_{\text{A}'}$ at the terminal allyl carbon atom C_{C} (*cis* to the PR_2 moiety) and selective NOE contacts (red) between the *syn/anti* and central allyl protons. There is no exchange of *syn* and *anti* protons at C_{A} . The selective *syn/anti* exchange indicates

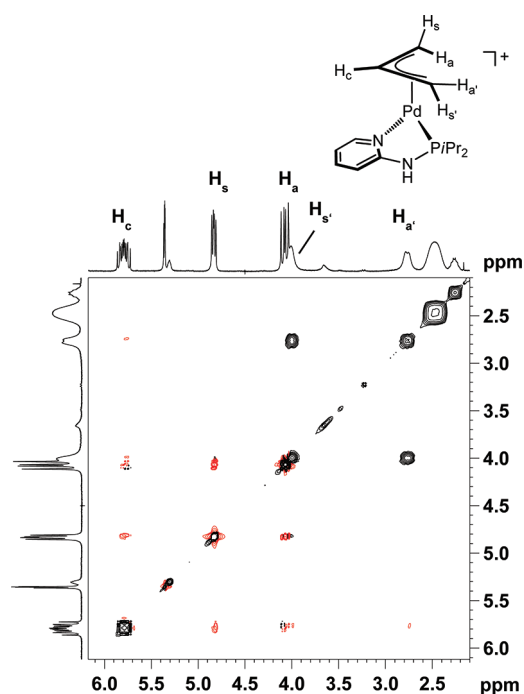
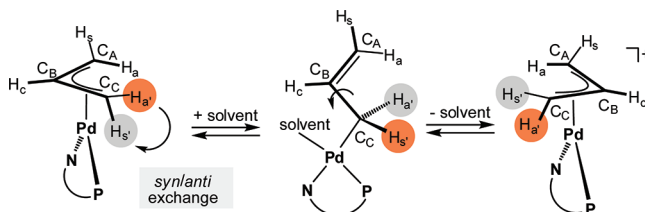


Figure 13. Section of a phase-sensitive 300 MHz ^1H , ^1H NOESY spectrum of $[\text{Pd}(\eta^3\text{-CH}_2\text{CHCH}_2)(\kappa^2(\text{P},\text{N})\text{-PN-}i\text{Pr})]\text{SbF}_6^-$ (**6b**) in CD_2Cl_2 at 25°C . The exchange cross-peaks between *syn/anti* protons are shown as black circles, whereas the NOE contacts between the corresponding *syn/anti* and central allyl protons are indicated in red.

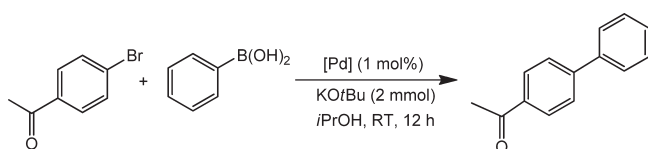
Scheme 6



that the η^3 – η^1 – η^3 isomerization follows a mechanism in which the Pd– C_{A} bond opens, forming an η^1 intermediate wherein the C_{B} – C_{C} bond rotates 180° , completed by re-formation of the η^3 -allyl with an interchange of $\text{H}_{\text{S}'}$ and $\text{H}_{\text{A}'}$ (Scheme 6). Importantly, the selective opening of the η^3 -allyl occurs *trans* to the phosphine. The η^3 – η^1 -allyl isomerization can be either under electronic control (the strongest donor stabilizes the terminal allyl carbon in pseudo-*trans* position) or under steric control (the largest ligand induces opening of the *cis*-positioned terminal allyl carbon).^{26,28} In the present case the isomerization is electronically controlled due to the much stronger *trans* influence of the phosphine moiety. The increased Pd– C_{A} bond length is also apparent in the crystal structures of **7b**, **8b**, and **9** (Table 1). It was found in several palladium complexes containing either bidentate PP and NN ligands with different phosphorus and nitrogen donor atoms,^{29,30} heterodifunctional ligands,^{31,32} or two different monodentate ligands^{33,34} that this isomerization is selective, involving opening of only one Pd–C bond of the allyl fragment.

b. Allyl Pseudorotation. The ligand dynamics in the palladium allyl EN (E = O, S, Se) complexes is clearly different from the

Table 1. Precatalyst Performance in the Suzuki–Miyaura Coupling of a Simple Substrate^a



| entry | [Pd] | yield (%) ^b |
|-------|--|------------------------|
| 1 | [Pd(η^3 -CH ₂ CHCH ₂)(PN-Ph)]SbF ₆ (6a) | 77 |
| 2 | [Pd(η^3 -CH ₂ CHCH ₂)(ON- <i>i</i> Pr)]SbF ₆ (10) | 96 |
| 3 | [Pd(η^3 -CH ₂ CHCH ₂)(SN-Ph)]SbF ₆ (14a) | traces |
| 4 | [Pd(η^3 -CHPhCHCH ₂)(PN-Ph)]SbF ₆ (8a) | 95 |
| 5 | [Pd(η^3 -CHPhCHCH ₂)(PN- <i>i</i> Pr)]SbF ₆ (8b) | 86 |
| 6 | [Pd(η^3 -CHPhCHCH ₂)(ON-Ph)]SbF ₆ (12a) | 96 |
| 7 | [Pd(η^3 -CHPhCHCH ₂)(ON- <i>i</i> Pr)]SbF ₆ (12b) | 96 |
| 8 | [Pd(η^3 -CHPhCHCH ₂)(SN-Ph)]SbF ₆ (16a) | 35 |
| 9 | [Pd(η^3 -CHPhCHCH ₂)(SN- <i>i</i> Pr)]SbF ₆ (16b) | traces |

^a Reaction conditions: aryl bromide (1.0 mmol), boronic acid (1.5 mmol), KOtBu (2.0 mmol), and catalyst (1 mol %). The reaction was stirred for 12 h.

^b Isolated yields, average of two runs.

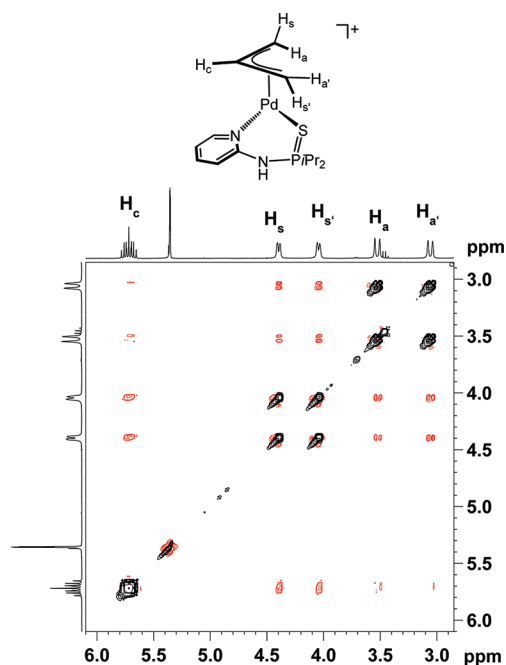


Figure 14. Section of a phase-sensitive 300 MHz ¹H,¹H NOESY spectrum of [Pd(η^3 -CH₂CHCH₂)(κ^2 (S,N)-SN-*i*Pr)]SbF₆ (**14b**) in CD₂Cl₂ at 25 °C. The exchange cross-peaks between *syn/syn'* and *anti/anti'* protons are shown as black circles, whereas the NOE contacts between the corresponding *syn/anti* and central allyl protons are indicated in red.

analogous PN compounds. A phase-sensitive 300 MHz ¹H,¹H NOESY spectrum of **14b** in CD₂Cl₂ at 25 °C is shown in Figure 14. In contrast to palladium allyl PN complexes, no η^3 - η^1 - η^3 isomerization takes place, as evident from the absence of any *syn/anti* exchange. Instead, an analysis of the 2D NMR data reveals selective *syn/syn'* and *anti/anti'* allyl proton exchange in this case. There are several reports of this

type of selective *syn/syn'* and *anti/anti'* exchange in Pd-allyl chemistry.^{22b,27} The fluxional process observed in these molecules, called *exo/endo* isomerization, effectively results in rotation of the allyl ligand in its own plane about the Pd- η^3 -allyl axis. The complex process may involve (a) dissociative (one must consider that the heterodifunctional EN ligand is *hemilabile*, resulting in the reversible decoordination of the E or N atoms) and/or (b) associative pathways (coordination of solvent or counterions present in solution). The latter pathway is usually called “apparent” allyl rotation. Both processes have the effect of switching the allylic termini with respect to their position relative to the EN donor set. In the present case, this process is solvent dependent and strongly facilitated in the presence of a coordinating solvent such as CH₃CN. We thus favor pathway (b) involving both reversible Pd-E and Pd-N bond cleavage with concomitant solvent coordination, as shown in Scheme 7 (see DFT calculations below).

c. DFT Studies. The mechanism of the dynamic processes described above for the allyl complexes **6b** and **14b** was investigated by means of DFT calculations.³⁵ For each complex, η^3 - η^1 - η^3 allyl isomerization and “apparent” allyl rotation (or η^3 -allyl pseudorotation) were compared in order to corroborate the experimental results. The energy profile calculated for the η^3 - η^1 - η^3 allyl isomerization process in [Pd(η^3 -CH₂CHCH₂)-(κ^2 (P,N)-PN-*i*Pr)]⁺ (**6b**⁺) is represented in Figure 15.

The entire path calculated for the process of *syn/anti* exchange in **6b**⁺ involves three steps. First there is coordination of one molecule of solvent (CH₃CN in the calculations), going from **A** to **B**, and, at the same time, the allyl ligand slips from η^3 - to η^1 -coordination. In **A** the acetonitrile molecule is away from the metal center with a Pd-N_{MeCN} separation of 4.42 Å, but once the transition state **TS_{AB}** is reached, that distance shortens to 2.34 Å, indicating an incipient bond, as shown by a Wiberg index (WI)³⁶ of 0.13. In **B**, formation of the Pd-N_{MeCN} bond is accomplished ($d_{\text{Pd-N}} = 2.13$ Å, WI = 0.21) and the allyl ligand has slipped to a η^1 -coordination, resulting from the breaking of the Pd-C bond involving the C atom *trans* to phosphorus ($d_{\text{Pd-C}} = 3.88$ Å). This cleavage of the Pd-C_{allyl} bond is already well advanced in **TS_{AB}**, as shown by a long distance (3.00 Å) and a Wiberg index indicative of a weak interaction (WI = 0.11).

The second step in the mechanism of *syn/anti* exchange in **6b**⁺ corresponds to rotation around the C-C bond in the η^1 -allyl ligand, from **B** to **C**. In the transition state (**TS_{BC}**) C-C rotation is halfway through, and the allyl ligand is in an upright position, with a Pd-C-C-C dihedral angle of 172°.

Finally, in the last step (from **C** to **D**) η^3 -allyl coordination is re-established with formation of the third Pd-C_{allyl} bond and loss of acetonitrile. In the transition state, **TS_{CD}**, formation of the new Pd-C bond is only incipient ($d_{\text{Pd-C}} = 2.99$ Å, WI = 0.12), while coordination of the solvent molecule is still significant ($d_{\text{Pd-N(MeCN)}} = 2.31$ Å, WI = 0.13). The overall result of the path, from **A** to **D**, is the exchange of the relative position of the allyl C-H bonds: the CH₂ *cis* to the phosphine retains its conformation along the path, while the central C-H bond and the CH₂ *trans* to the P atom exchange from one side of the coordination plane in **A** to the other, in **D**. Naturally, **A** and **D** are isoenergetic, for practical purposes.

In the mechanism discussed above, coordination of a solvent molecule provides the fourth ligand necessary to maintain the coordination number and the square-planar geometry characteristic of Pd(II) complexes in the η^1 -allyl intermediates, **B** and **C**, giving rise to a smooth process with a maximum energy barrier of

Scheme 7

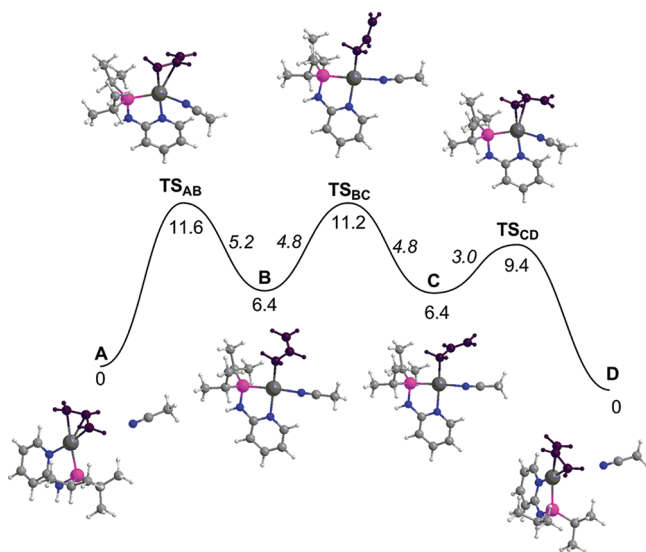
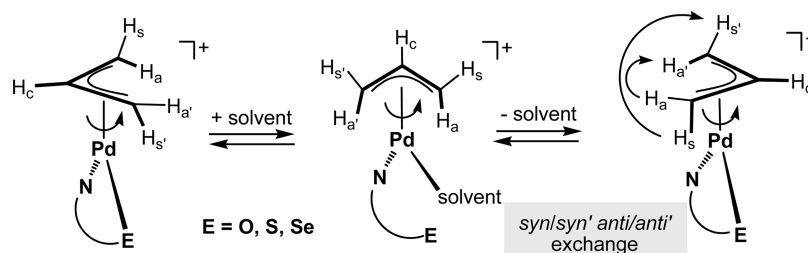


Figure 15. Energy profile (in kcal/mol) for the solvent-assisted (CH_3CN) η^3 - η^1 - η^3 allyl isomerization in $[\text{Pd}(\eta^3\text{-CH}_2\text{CHCH}_2)(\kappa^2(P,N)\text{-PN-}i\text{Pr})]^+$ ($6b^+$). The allyl ligand is darkened to highlight the fluxional process, and the numbers in italics indicate energy barriers.

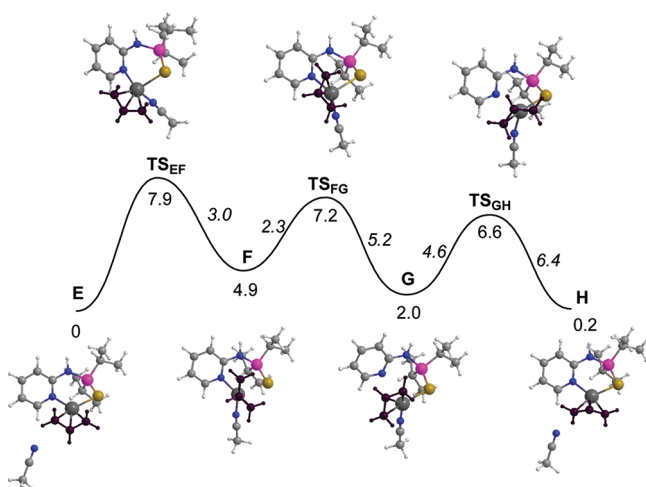
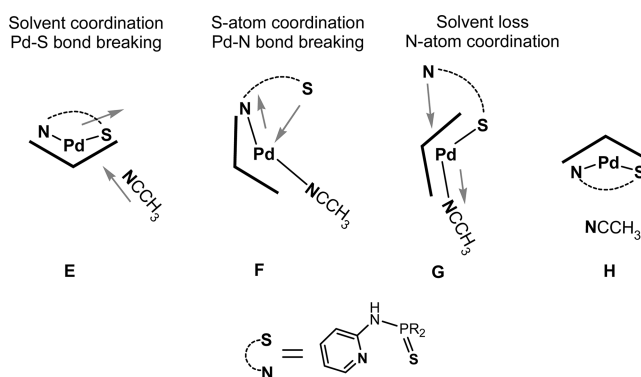


Figure 16. Energy profile (in kcal/mol) calculated for the solvent-assisted (CH_3CN) η^3 -allyl pseudorotation in $[\text{Pd}(\eta^3\text{-CH}_2\text{CHCH}_2)(\kappa^2(S,N)\text{-SN-}i\text{Pr})]^+$ ($14b^+$). The allyl ligand is darkened to highlight the fluxional process, and the numbers in italics indicate energy barriers.

Scheme 8



$11.6 \text{ kcal mol}^{-1}$, in good accordance with the fluxional process observed in the NMR (see above).

The mechanism of “apparent” allyl rotation was also explored for complex $6b^+$, and the corresponding energy profile is presented as Supporting Information (Figure S13). That mechanism is equivalent, in its general features, to the one obtained for complex $14b^+$, discussed below. Interestingly, the energy barrier calculated for complex $6b^+$ ($19.3 \text{ kcal mol}^{-1}$, see Figure S13) indicates that η^3 - η^1 - η^3 allyl isomerization is clearly the most favorable mechanism for that species, in agreement with the experimental data.

The energy profile calculated for the mechanism of η^3 -allyl pseudorotation in complex $[\text{Pd}(\eta^3\text{-CH}_2\text{CHCH}_2)(\kappa^2(S,N)\text{-SN-}i\text{Pr})]^+$ ($14b^+$) is represented in Figure 16.

The mechanism obtained for η^3 -allyl pseudorotation in $14b^+$ comprises three steps. First, there is coordination of one molecule of solvent with simultaneous breakage of the Pd–S bond, from E to F. In the corresponding transition state (TS_{EF}) cleavage of the Pd–S bond is already apparent with a distance (2.58 \AA) longer than the one presented in the reactant, E (2.41 \AA), indicating the weakening of the corresponding interaction, WI = 0.27 (E) and 0.15 (TS_{EF}). On the other hand, coordination of the acetonitrile molecule is also evident in TS_{EF} with a Pd–N_{MeCN} distance of 2.43 \AA , indicative of incipient bond formation (WI = 0.11).

The second step in the mechanism corresponds to exchange between N- and S-coordination of the SN-*i*Pr ligand, from F to G, respectively. The Pd–N interaction goes from a clear bond in F ($d_{\text{Pd-N(py)}} = 2.20 \text{ \AA}$, WI = 0.17) to a negligible interaction in G ($d_{\text{Pd-N(py)}} = 3.12 \text{ \AA}$, WI = 0.02), while the opposite happens with the Pd–S bond: nonexistent in F ($d_{\text{Pd-S}} = 2.84 \text{ \AA}$, WI = 0.06) and full coordination in G ($d_{\text{Pd-S}} = 2.43 \text{ \AA}$, WI = 0.28). The corresponding transition state, TS_{FG} , presents an intermediate situation with the Pd–N bond considerably weakened

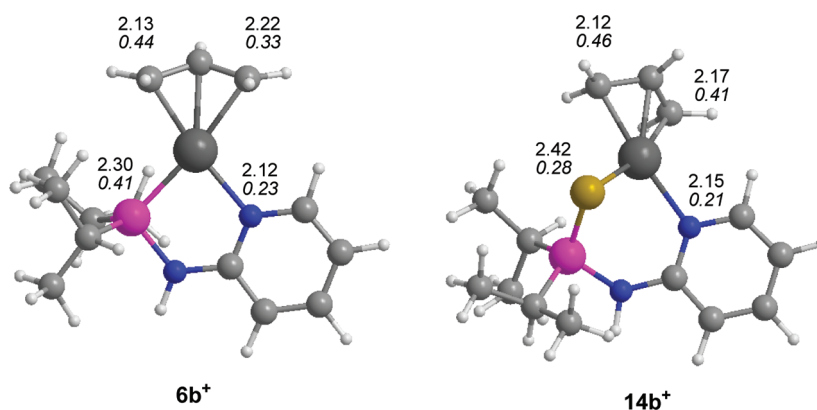


Figure 17. Relevant coordination distances (Å) and Wiberg indices (in italics) for complexes $[\text{Pd}(\eta^3\text{-CH}_2\text{CHCH}_2)(\kappa^2(\text{P},\text{N})\text{-PN-}i\text{Pr})]^+$ ($6b^+$) and $[\text{Pd}(\eta^3\text{-CH}_2\text{CHCH}_2)(\kappa^2(\text{S},\text{N})\text{-SN-}i\text{Pr})]^+$ ($14b^+$).

($d_{\text{Pd-N(py)}} = 2.47$ Å, WI = 0.08) and formation of the new Pd–S bond ($d_{\text{Pd-S}} = 2.62$ Å, WI = 0.15) already evident.

In the final step of the mechanism there is coordination of the N atom belonging to the pyridine ring of the SN-*i*Pr ligand, with concomitant loss of the solvent molecule, from G to H. This process is only incipient in the corresponding transition state, TS_{GH} , with a very weak Pd–N_{py} interaction ($d_{\text{Pd-N(py)}} = 2.56$ Å, WI = 0.07) and the acetonitrile molecule still moderately bound to the metal ($d_{\text{Pd-N(MeCN)}} = 2.35$ Å, WI = 0.13).

The mechanism obtained for η^3 -allyl pseudorotation in $14b^+$ is represented in Scheme 8 in a simplified way, highlighting solvent assistance. The overall result of that fluxional process is a 180° rotation of the allyl ligand in its own plane, that is, a *syn/syn'* and *anti/anti'* exchange, from E to H, two conformers practically isoenergetic with cation $14b^+$ (within 0.2 kcal mol⁻¹). Solvent plays a crucial role in the fluxional process, providing the fourth ligand necessary to maintain the coordination number and the square-planar geometry around the metal in the intermediates, F and G, avoiding, thus, the existence of pseudotetrahedral intermediates or transition states, unfavorable in a d⁸ metal center such as Pd(II). The maximum barrier calculated for the allyl pseudorotation is rather small (7.9 kcal mol⁻¹), in good agreement with the NMR results (see above).

The mechanism of $\eta^3\text{-}\eta^1\text{-}\eta^3$ allyl isomerization was also investigated for complex $14b^+$, and the corresponding energy profile is presented as Supporting Information (Figure S14). The energy barrier calculated for that process (14.8 kcal mol⁻¹) is higher than the one obtained for the alternative path, i.e., η^3 -allyl rotation, indicating the latter as the most favorable process in the case of complex $14b^+$, in agreement with the experimental data. The mechanism obtained for $\eta^3\text{-}\eta^1\text{-}\eta^3$ allyl isomerization in $14b^+$ is equivalent, in its general features, to the one calculated for complex $6b^+$, discussed above (Figure 15).

The reason for the different paths observed for the fluxional processes of the PN complexes, compared to the EN analogues (E = O, S, Se), can be traced to the nature of the Pd–P/E bond and to the *trans* influence of this donor atom.

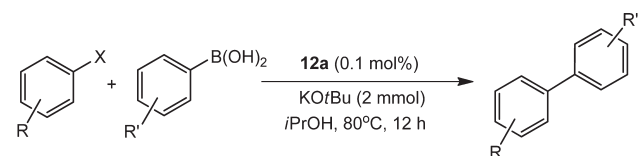
Comparing cations $6b^+$ and $14b^+$ (see Figure 17), the differences in the coordination environment around the metal are evident. On one hand, the Pd–P bond in $6b^+$ is considerably stronger than the Pd–S bond in $14b^+$, as shown by the corresponding Wiberg indices in Figure 17. Naturally, this makes any path involving decoordination of the PN ligand, such as the one obtained for η^3 -allyl pseudorotation, less favorable than an

equivalent mechanism with the SN ligand. On the other hand, a P-donor atom has a much stronger *trans* influence than an S-donor atom, and thus, the weakening of the corresponding *trans* Pd–C_{allyl} bond is considerably more effective in the case of the PN ligand. As a consequence, the difference between the two Pd–C bonds involving the terminal allyl C atoms is enhanced in the case of $6b^+$, resulting in an asymmetry on the allyl coordination that facilitates the $\eta^3\text{-}\eta^1$ isomerization process in this species, compared with the SN complex.

Suzuki–Miyaura Cross-Coupling Reactions. Palladium complexes containing allyl ligands were shown to be excellent catalysts for the Suzuki–Miyaura cross coupling.^{34,37} On the basis of these findings we were interested in whether our palladium complexes containing EN ligands exhibit similar reactivities in C–C bond coupling reactions. Accordingly, we investigated the activity of several new palladium allyl complexes as catalysts for the coupling of aryl bromides with aryl boronic acids.

In general, the coupling reaction is more efficient if complexes **10**, **8a**, **12a**, and **12b**, with PN-Ph and ON-Ph ligands, are used (Table 1, entries 2, 4, 6, and 7) instead of complexes with SN ligands, possibly due to metal poisoning through the sulfide group. While it is difficult to establish any clear trends in the catalytic activity of these particular complexes on these preliminary data, complexes **8a**, **12a**, and **12b**, featuring cinnamyl ligands, show higher activity than the other complexes, on average. This reactivity trend suggests that substitution at the terminal position of the allyl moiety increases the dissymmetry of the allyl scaffold bound to the palladium and renders the catalyst more active. Similar effects have been observed by others.³⁷ For substrate screening we thus focused on the cinnamyl complex **12b** as precatalyst. The results of this study are summarized in Table 2. Under classical conditions, complex **12b** was shown to be promising, although it does not surpass the activities of other related catalysts.^{37a,38} At 80 °C, a catalyst loading of 0.1 mol % was sufficient to observe quantitative conversion of the starting materials into the expected biaryl products (entries 1–10). On the other hand, with 4-chloroacetophenone and phenylboronic acid, even with a catalyst loading of 1 mol %, the yield of 4-acetylbiphenyl was rather low (entry 11). Though these results do not compare with those obtained by the group of Nolan³⁷ using palladium allyl complexes with N-heterocyclic carbenes as coligands, these catalysts do prove to be very efficient.

Table 2. Suzuki–Miyaura Cross-Coupling of Aryl Halides with Arylboronic Acids Catalyzed by $[\text{Pd}(\eta^3\text{-CHPhCH}_2\text{-}(\kappa^2(\text{O},\text{N})\text{-ON-Ph}))\text{SbF}_6$ (12a**)^{a,b,c,d}**



| entry | Ar-X | Ar'-B(OH) ₂ | product | yield (%) ^b |
|-------|------|------------------------|---------|------------------------|
| 1 | | | | 96 |
| 2 | | | | 96 |
| 3 | | | | 96 |
| 4 | | | | 96 ^c |
| 5 | | | | 97 |
| 6 | | | | 95 |
| 7 | | | | 97 |
| 8 | | | | 97 |
| 9 | | | | 96 |
| 10 | | | | 97 |
| 11 | | | | 25 ^d |

^a Reaction conditions: aryl halide (1.0 mmol), boronic acid (1.5 mmol), KOtBu (2.0 mmol), and catalyst (0.1 mol %). The reaction was stirred for 12 h. ^b Isolated yields, average of two runs. ^c Catalyst loading 0.01 mol %. ^d Catalyst loading 1 mol %

CONCLUSION

In summary, we have shown that cationic palladium allyl complexes of the type $[\text{Pd}(\eta^3\text{-allyl})(\kappa^2(\text{E},\text{N})\text{-EN-chelate})]^+$ are obtained in high yields from the reaction of the chloro-bridged palladium allyl dimers $[\text{Pd}(\eta^3\text{-allyl})(\mu\text{-Cl})_2]$ with several hetero-difunctional EN (E = P, O, S, Se) ligands in the presence of AgSbF_6 or AgCF_3SO_3 . These complexes were studied by one- and two-dimensional NMR techniques together with X-ray structure determinations and DFT calculations. Variable-temperature and phase-sensitive ^1H , ^1H NOESY NMR measurements reveal that both allyl and EN ligands exhibit fluxional behavior. In the case of palladium PN complexes η^3 to η^1 isomerization takes

place by opening of the η^3 -allyl group selectively at the *trans* position with respect to the phosphorus center, while for EN (E = O, S, Se) complexes an “apparent” allyl rotation is observed proceeding with Pd–E and Pd–N bond breaking. Thus, the Pd–P and Pd–N bonds are stronger and the Pd–E and Pd–N bonds are weaker than the allylic Pd–C bonds, respectively. DFT calculations indicate that both isomerization processes are solvent assisted, corroborating the NMR experiments. The palladium allyl complexes proved to be active as catalysts for Suzuki–Miyaura coupling reactions, representing an interesting alternative to existing catalytic palladium allyl systems due to the simplicity and modularity as their synthesis is concerned.

EXPERIMENTAL SECTION

General Procedures. All manipulations were performed under an inert atmosphere of argon by using Schlenk techniques. The solvents were purified according to standard procedures.³⁹ The ligands *N*-diphenylphosphino-2-aminopyridine (PN-Ph) (**1a**),⁴⁰ *N*-diisopropylphosphino-2-aminopyridine (PN-*i*Pr) (**1b**), *N*-(2-pyridinyl)aminodiphenylphosphine sulfide (SN-Ph) (**3a**), *N*-(2-pyridinyl)aminodiisopropylphosphine sulfide (SN-*i*Pr) (**3b**), *N*-(2-pyridinyl)aminodiphenylphosphine selenide (SeN-Ph) (**4a**),⁴¹ and *N*-(2-pyridinyl)aminodiisopropylphosphine selenide (SN-*i*Pr) (**4b**) and the $[\text{Pd}(\eta^3\text{-allyl})(\mu\text{-Cl})_2]$ dimers (**5a–d**)⁴² were prepared according to the literature. The deuterated solvents were dried over 4 Å molecular sieves. ^1H , $^{13}\text{C}\{^1\text{H}\}$, and $^{31}\text{P}\{^1\text{H}\}$ NMR spectra were recorded on Bruker AVANCE-250 and AVANCE-300 DPX spectrometers and were referenced to SiMe_4 and H_3PO_4 (85%), respectively. ^1H and $^{13}\text{C}\{^1\text{H}\}$ NMR signal assignments were confirmed by ^1H -COSY, 13S-DEPT, and HMQC (^1H – ^{13}C) experiments. For the ^1H , ^1H NOESY experiments a mixing time of 1 s was used.

***N*-(2-Pyridinyl)aminodiphenylphosphine Oxide (ON-Ph) (2a).** A solution of *N*-(2-pyridinyl)aminodiphenylphosphine (PN-Ph) (**1a**) (3.01 g, 10.8 mmol) in THF was cooled to 5 °C, and aqueous H_2O_2 (30 w/w, 2.18 mL, 32.5 mmol) was slowly added. After the solution reached room temperature the reaction mixture was stirred for 30 min. The solvent was then evaporated, and the crude solid product was purified with column chromatography using THF and silica gel. Yield: 2.81 g (88%). Anal. Calcd for $\text{C}_{17}\text{H}_{15}\text{N}_2\text{OP}$: C, 69.38; H, 5.14; N, 9.52. Found: C, 69.30; H, 5.20; N, 9.62. ^1H NMR (δ , CDCl_3 , 20 °C): 7.91–7.83 (m, 4H, Ph^{2,6}), 7.65 (d, $J = 4.5$ Hz, py⁶), 7.54–7.30 (m, 8H, Ph^{3,4,5}, py⁵, NH), 6.98 (d, 8.3 Hz, py³), 6.63 (m, py⁴). $^{13}\text{C}\{^1\text{H}\}$ NMR (δ , CDCl_3 , 20 °C): 154.1 (s, py²), 147.9 (s, py⁶), 137.9 (s, py⁴), 132.3 (s, Ph⁴), 131.9 (d, $J = 10.1$ Hz, Ph^{2,6}), 131.7 (d, $J = 129.2$ Hz, Ph¹), 128.7 (d, $J = 13.2$ Hz, Ph^{3,5}), 117.0 (s, py⁵), 112.0 (s, py³). $^{31}\text{P}\{^1\text{H}\}$ NMR (δ , CD_2Cl_2 , 20 °C): 31.9.

***N*-(2-Pyridinyl)aminodiisopropylphosphine Oxide (ON-*i*Pr) (2b).** This ligand was prepared analogously to **2a** with **1b** (5.15 g, 24.5 mmol) and aqueous H_2O_2 (30 w/w, 4.95 mL, 73.5 mmol) as the starting materials. Yield: 5.09 g (92%). Anal. Calcd for $\text{C}_{11}\text{H}_{19}\text{N}_2\text{OP}$: C, 58.39; H, 8.46; N, 12.38. Found: C, 58.42; H, 8.21; N, 12.30. ^1H NMR (δ , CD_2Cl_2 , 20 °C): 8.06 (d, $J = 4.5$ Hz, py⁶), 7.88 (s, NH), 7.49 (t, $J = 7.2$ Hz, py⁴), 7.09 (d, $J = 8.3$ Hz, py³), 6.74 (dd, $J = 6.6$ Hz, $J = 5.6$ Hz, py⁵), 2.69–2.42 (dh, $J = 2.0$ Hz, $J = 7.2$ Hz, 2H, CH(CH₃)₂), 1.32–1.10 (m, 12H, CH(CH₃)₂). $^{13}\text{C}\{^1\text{H}\}$ NMR (δ , CD_2Cl_2 , 20 °C): 156.2 (s, py²), 147.3 (s, py⁶), 137.5 (s, py⁴), 115.3 (s, py⁵), 111.4 (d, $J = 5.5$ Hz, py³), 26.7 (d, $J = 79.8$ Hz, CH(CH₃)₂), 15.8 (d, $J = 3.4$ Hz, CH(CH₃)₂), 15.5 (s, CH(CH₃)₂). $^{31}\text{P}\{^1\text{H}\}$ NMR (δ , CD_2Cl_2 , 20 °C): 70.9.

$[\text{Pd}(\eta^3\text{-CH}_2\text{CHCH}_2)(\text{PN-Ph})\text{SbF}_6$ (6a). A solution of **5a** (92 mg, 0.25 mmol) and **1a** (140 mg, 0.50 mmol) in 10 mL of CH_2Cl_2 was treated with AgSbF_6 (172 mg, 0.50 mmol) and stirred for 30 min. Solid materials (AgCl) were then removed by filtration over Celite, and the solvent was removed under reduced pressure to give a pale yellow solid, which was washed twice with diethyl ether (10 mL) and dried under

vacuum. Yield: 322 mg (97%). Anal. Calcd for $C_{20}H_{20}F_6N_2PPdSb$: C, 36.31; H, 3.05; N, 4.23. Found: C, 36.42; H, 3.21; N, 3.00. 1H NMR (δ , CD_2Cl_2 , 20 °C): 8.46 (d, $J = 5.6$ Hz, 1H, py^6), 7.81 (t, $J = 7.9$ Hz, 1H, py^4), 7.75–7.44 (m, 10H, Ph), 7.28 (d, $J = 8.5$ Hz, 1H, py^3), 7.02–6.89 (m, 2H, NH, py^5), 6.24–5.62 (m, 1H, CH), 4.91 (t, $J = 5.8$ Hz, 1H, CH), 4.21 (dd, $J = 10.0$ Hz, 14.0 Hz, 1H, CH), 4.12 (d, $J = 6.5$ Hz, 1H, CH), 2.96 (d, $J = 12.2$ Hz, 1H, CH). $^{13}C\{^1H\}$ NMR (δ , CD_2Cl_2 , 20 °C): 160.0 (d, $J_{CP} = 13.4$ Hz, py^2), 153.4 (d, $J_{CP} = 2.1$ Hz, py^6), 141.6 (s, py^4), 132.5 (s, Ph), 131.9 (d, $J_{CP} = 16.1$ Hz, Ph), 131.7 (d, $J = 15.6$ Hz, Ph), 129.5 (d, $J = 3.7$ Hz, Ph), 129.4 (d, $J = 3.8$ Hz, Ph), 123.2 (d, $J_{CP} = 6.0$ Hz, CH), 117.4 (s, py^5), 112.7 (d, $J_{CP} = 7.2$ Hz, py^3), 82.2 (d, $J_{CP} = 31.4$ Hz, CH_2), 52.1 (d, $J_{CP} = 3.9$ Hz, CH_2). $^{31}P\{^1H\}$ NMR (δ , CD_2Cl_2 , 20 °C): 76.1.

[Pd(η^3 -CH₂CHCH₂)(PN-*i*Pr)]SbF₆ (6b). This complex was prepared analogously to complex 6a using 5a (184 mg, 0.50 mmol), 1b (220 mg, 1.05 mmol), and AgSbF₆ (343 mg, 1 mmol) as starting materials. Yield: 585 mg (98%). Anal. Calcd for $C_{14}H_{24}F_6N_2PPdSb$: C, 28.33; H, 4.08; N, 4.72. Found: C, 28.20; H, 4.11; N, 4.65. 1H NMR (δ , CD_2Cl_2 , -40 °C): 8.38 (d, $J = 5.6$ Hz, 1H, py^6), 7.76 (t, $J = 7.8$ Hz, 1H, py^3), 7.23 (d, $J = 8.5$ Hz, 1H, py^4), 6.86 (t, $J = 7.0$ Hz, 1H, py^5), 6.34 (s, 1H, NH), 6.03–5.51 (m, 1H, CH), 4.81 (dd, $J = 7.8$, 5.3 Hz, 1H, CH), 4.05 (dd, $J = 14.1$, 9.4 Hz, 1H, CH), 3.92 (d, $J = 9.4$ Hz, 1H, CH), 2.76 (d, $J = 7.8$ Hz, 1H, CH), 2.60–2.29 (m, 2H, CH), 1.19 (dd, $J = 17.6$, 8.8 Hz, 12H, CH_3). $^{13}C\{^1H\}$ NMR (δ , CD_2Cl_2 , 20 °C): 161.7 (d, $J_{CP} = 10.0$ Hz, py^2), 153.4 (s, py^6), 141.2 (s, py^4), 121.9 (d, $J_{CP} = 5.5$ Hz, CH), 116.6 (s, py^5), 112.2 (d, $J_{CP} = 6.1$ Hz, py^3), 82.7 (d, $J_{CP} = 29.6$ Hz, CH_2), 46.4 (d, $J_{CP} = 3.1$ Hz, CH_2), 27.3 (d, $J_{CP} = 25.7$ Hz, CH), 17.9 (d, $J_{CP} = 7.9$ Hz, CH_3), 16.8 (s, CH_3). $^{31}P\{^1H\}$ NMR (δ , CD_2Cl_2 , 20 °C): 127.1.

[Pd(η^3 -CH₂CMeCH₂)(PN-Ph)]SbF₆ (7a). This complex was prepared analogously to complex 6a using 5b (100 mg, 0.25 mmol), 1a (140 mg, 0.50 mmol), and AgSbF₆ (172 mg, 0.50 mmol) as starting materials. Yield: 326 mg (95%). Anal. Calcd for $C_{21}H_{22}F_6N_2PPdSb$: C, 37.34; H, 3.28; N, 4.15. Found: C, 37.45; H, 3.21; N, 4.45. 1H NMR (δ , CD_2Cl_2 , 20 °C): 8.48 (d, $J = 4.7$ Hz, 1H, py^6), 7.88–7.5 (m, 10H, py, Ph), 7.28 (d, $J = 10.7$ Hz, 2H), 7.07 (s, 1H, NH), 6.99–6.89 (m, 1H, py^5), 4.66 (s, 1H, CH), 4.00 (d, $J = 10.1$ Hz, 1H, CH), 3.89 (s, 1H, CH), 2.86 (s, 1H, CH), 2.13 (s, 3H, CH_3). $^{13}C\{^1H\}$ NMR (δ , CD_2Cl_2 , 20 °C): 160.1 (d, $J_{CP} = 13.6$ Hz, py^2), 153.2 (d, $J_{CP} = 2.3$ Hz, py^6), 141.5 (s, py^4), 138.9 (d, $J_{CP} = 5.8$, CCH_3), 132.5 (d, $J_{CP} = 2.4$ Hz, Ph), 132.4 (d, $J_{CP} = 2.4$ Hz, Ph), 131.9 (d, $J_{CP} = 16.4$ Hz, Ph), 131.6 (d, $J_{CP} = 15.7$ Hz, Ph), 131.0 (d, $J_{CP} = 11.3$, Ph), 129.4 (d, $J_{CP} = 11.7$ Hz, Ph), 128.5.0 (d, $J = 13.4$, Ph), 117.3 (s, py^5), 112.7 (d, $J_{CP} = 7.1$ Hz, py^3), 79.9 (d, $J_{CP} = 33.1$ Hz, CH_2), 52.6 (s, CH_2), 23.9 (s, CH_3). $^{31}P\{^1H\}$ NMR (δ , CD_2Cl_2 , 20 °C): 89.3.

[Pd(η^3 -CH₂CMeCH₂)(PN-*i*Pr)]SbF₆ (7b). This complex was prepared analogously to complex 6a using 5b (196 mg, 0.50 mmol), 1b (220 mg, 1.05 mmol), and AgSbF₆ (343 mg, 1 mmol) as starting materials. Yield: 600 mg (98%). Anal. Calcd for $C_{15}H_{26}F_6N_2PPdSb$: C, 29.66; H, 4.31; N, 4.61. Found: C, 29.68; H, 4.21; N, 4.70. 1H NMR (δ , acetone-*d*₆, 20 °C): 8.62 (d, $J = 5.8$ Hz, 1H, py^6), 7.89 (t, $J = 7.4$ Hz, 2H, NH, py^3), 7.24 (d, $J = 8.5$ Hz, 1H, py^4), 6.95 (t, $J = 6.5$ Hz, 1H, py^5), 4.83 (d, $J = 3.0$ Hz, 1H, CH), 4.07 (d, $J = 9.5$ Hz, 1H, CH), 3.94 (s, 1H, CH), 2.87 (s, 1H, CH), 2.72–2.45 (m, 1H, CH), 2.09 (s, 2H, CH_3), 1.37–1.13 (m, CH_3). $^{13}C\{^1H\}$ NMR (δ , acetone-*d*₆, 20 °C): 162.4 (s, py^2), 153.8 (d, $J_{CP} = 1.9$ Hz, py^6), 141.3 (s, py^4), 137.3 (d, $J_{CP} = 5.3$ Hz, CCH_3), 116.5 (s, py^5), 111.8 (d, $J_{CP} = 6.1$ Hz, py^3), 80.9 (d, $J_{CP} = 30.9$ Hz, CH_2), 47.6 (d, $J_{CP} = 2.6$ Hz, CH_2), 26.8 (d, $J_{CP} = 25.2$ Hz, CH), 23.1 (s, CH_3), 17.5 (dd, $J_{CP} = 22.6$, 8.0 Hz, CH_3), 16.5 (d, $J_{CP} = 12.6$ Hz, CH_3). $^{31}P\{^1H\}$ NMR (δ , acetone-*d*₆, 20 °C): 126.5.

[Pd(η^3 -CHPhCHCH₂)(PN-Ph)]SbF₆ (8a). This complex was prepared analogously to complex 6a using 5d (129 mg, 0.25 mmol), 1a (140 mg, 0.50 mmol), and AgSbF₆ (172 mg, 0.50 mmol) as starting materials. Yield: 369 mg (100%). Anal. Calcd for $C_{26}H_{24}F_6N_2PPdSb$: C, 42.34; H, 3.28; N, 3.80. Found: C, 42.42; H, 3.18; N, 3.70. 1H NMR

(δ , CD_2Cl_2 , 20 °C): 7.80–7.36 (m, 17H, py, Ph), 7.27 (d, $J = 8.4$ Hz, 1H, py^3), 6.90 (d, $J = 5.3$ Hz, 1H, NH), 6.53 (t, $J = 6.5$ Hz, 1H, py^5), 6.36 (m, 1H, CH), 5.49 (dd, $J = 13.3$, 10.3 Hz, 1H, CH), 3.70–3.50 (m, 2H, CH_2). $^{13}C\{^1H\}$ NMR (δ , CD_2Cl_2 , 20 °C): 160.5 (d, $J_{CP} = 14.0$ Hz, py^2), 146.8 (s, py^6), 141.2 (s, py^4), 134.8 (d, $J_{CP} = 6.1$ Hz, Ph), 132.4 (d, $J_{CP} = 2.6$ Hz, Ph), 132.0 (s, Ph), 131.7 (s, Ph), 129.9 (d, $J_{CP} = 2.2$ Hz, Ph), 129.5 (s, Ph), 129.3 (s, Ph), 128.0 (d, $J_{CP} = 3.7$ Hz, Ph), 116.6 (s, py^5), 115.0 (d, $J_{CP} = 6.6$ Hz, CH), 112.5 (d, $J_{CP} = 7.1$ Hz, py^3), 100.5 (d, $J_{CP} = 28.8$ Hz, CHPh), 50.6 (d, $J_{CP} = 3.9$ Hz, CH_2). $^{31}P\{^1H\}$ NMR (δ , CD_2Cl_2 , 20 °C): 90.6.

[Pd(η^3 -CHPhCHCH₂)(PN-*i*Pr)]SbF₆ (8b). This complex was prepared analogously to complex 6a using 5d (129 mg, 0.25 mmol), 1b (110 mg, 0.52 mmol), and AgSbF₆ (172 mg, 0.50 mmol) as starting materials. Yield: 328 mg (98%). Anal. Calcd for $C_{20}H_{28}F_6N_2PPdSb$: C, 35.88; H, 4.21; N, 4.18. Found: C, 35.92; H, 4.11; N, 4.30. 1H NMR (δ , CD_2Cl_2 , 20 °C): 7.69–7.41 (m, 6H, py, Ph), 7.17 (d, $J = 8.4$ Hz, 1H, Ph), 6.84 (d, $J = 5.4$ Hz, 1H, py), 6.48 (t, $J = 6.5$ Hz, 1H, py), 6.37 (s, 1H, NH), 6.18 (dd, $J = 13.4$, 9.6 Hz, 1H, CH), 5.39–5.29 (m, 1H, CH), 4.13–2.87 (m, 2H, CH_2), 2.49 (dd, $J = 13.6$, 6.8 Hz, 2H, CH), 1.34–1.11 (m, 12H, CH_3). $^{13}C\{^1H\}$ NMR (δ , CD_2Cl_2 , 20 °C): 162.0 (d, $J = 10.5$ Hz, py^2), 146.8 (s, py^6), 140.93 (s, py^4), 135.0 (d, $J_{CP} = 5.6$ Hz, Ph), 129.8 (d, $J_{CP} = 2.0$ Hz, Ph), 129.3 (d, $J_{CP} = 2.6$ Hz, Ph), 127.7 (d, $J_{CP} = 3.4$ Hz, Ph), 116.0 (s, py^5), 113.9 (d, $J_{CP} = 6.1$ Hz, CH), 112.0 (d, $J_{CP} = 5.8$ Hz, py^3), 100.8 (d, $J_{CP} = 27.2$ Hz, CHPh), 44.9 (d, $J_{CP} = 2.8$ Hz, CH_2), 27.5 (s, CH), 19.2–16.4 (m, CH_3). $^{31}P\{^1H\}$ NMR (δ , CD_2Cl_2 , 20 °C): 129.1.

[Pd(η^3 -CHPhCHCHPh)(PN-*i*Pr)]SbF₆ (9). This complex was prepared analogously to complex 6a using 5e (167 mg, 0.25 mmol), 1b (110 mg, 0.50 mmol), and AgSbF₆ (172 mg, 0.50 mmol) as starting materials. Yield: 325 mg (87%). Anal. Calcd for $C_{26}H_{32}F_6N_2PPdSb$: C, 41.88; H, 4.33; N, 3.76. Found: C, 41.92; H, 4.27; N, 3.50. 1H NMR (δ , CD_2Cl_2 , 20 °C): 7.87–7.20 (m, 12H, $py^{6,3}$, Ph), 7.09 (d, $J = 8.6$ Hz, 1H, py^4), 6.94–6.59 (m, 1H, CH), 6.44 (t, $J = 3.0$ Hz, 1H, py^5), 6.00 (s, 1H, NH), 5.51 (d, $J = 13.4$ Hz, 1H, CH), 4.93 (d, $J = 11.4$ Hz, CH), 2.48–2.24 (m, 2H, CH), 1.52–0.60 (m, 12H, CH_3). $^{13}C\{^1H\}$ NMR (δ , CD_2Cl_2 , 20 °C): 161.7 (d, $J_{CP} = 10.4$ Hz, py^2), 146.7 (s, py^6), 140.9 (s, py^4), 139.0 (d, $J_{CP} = 2.1$ Hz, Ph), 135.0 (d, $J_{CP} = 5.9$ Hz, Ph), 130.0 (d, $J_{CP} = 2.0$ Hz, Ph), 129.6 (d, $J_{CP} = 2.6$ Hz, Ph), 129.4 (d, $J_{CP} = 1.4$ Hz, Ph), 128.5–128.0 (Ph), 127.1 (d, $J_{CP} = 3.0$ Hz, Ph), 115.8 (s, py^5), 112.5 (d, $J_{CP} = 6.0$ Hz, CH), 112.0 (d, $J_{CP} = 5.2$ Hz, py^3), 97.1 (d, $J_{CP} = 24.9$ Hz, CHPh), 68.8 (d, $J_{CP} = 5.5$ Hz, CH), 27.3 (d, $J_{CP} = 22.6$ Hz, CH), 25.0 (d, $J_{CP} = 22.5$ Hz, CH), 17.4 (d, $J_{CP} = 4.9$ Hz, CH_3), 15.3 (d, $J_{CP} = 4.2$ Hz, CH_3). $^{31}P\{^1H\}$ NMR (δ , CD_2Cl_2 , 20 °C): 118.6.

[Pd(η^3 -CH₂CHCH₂)(ON-*i*Pr)]SbF₆ (10). This complex was prepared analogously to complex 6a using 5a (184 mg, 0.50 mmol), 2b (237 mg, 1.05 mmol), and AgSbF₆ (343 mg, 1.00 mmol) as starting materials. Yield: 540 mg (89%). Anal. Calcd for $C_{14}H_{24}F_6N_2OPPdSb$: C, 27.59; H, 3.97; N, 4.60. Found: C, 27.55; H, 4.07; N, 4.50. 1H NMR (δ , CD_2Cl_2 , 20 °C): 8.23 (d, $J = 4.2$ Hz, 1H, py^6), 7.86 (t, $J = 7.31$ Hz, 1H, py^3), 7.31 (d, $J = 7.8$ Hz, 1H, py^4), 7.09 (t, $J = 5.81$ Hz, 1H, py^5), 6.32 (d, $J = 11.1$ Hz, 1H, NH), 5.88–5.70 (m, 1H, CH), 4.18 (bs, 1H, CH), 3.90 (bs, 1H, CH), 3.62 (bs, 1H, CH), 3.22 (bs, 1H, CH), 2.37 (d, $J = 6.8$ Hz, 2H, CH), 1.38–1.08 (m, 12H, CH_3). $^{13}C\{^1H\}$ NMR (δ , CD_2Cl_2 , 20 °C): 155.4 (s, py^2), 152.1 (s, py^6), 141.4 (s, py^4), 119.5 (s, CH), 118.7 (s, py^3), 116.0 (s, py^5), 62.8 (s, CH_2), 58.9 (s, CH_2), 16.4 (d, $J_{CP} = 82.9$ Hz, CH), 15.1 (d, $J_{CP} = 3.2$ Hz, CH_3), 14.7 (s, CH_3). $^{31}P\{^1H\}$ NMR (δ , CD_2Cl_2 , 20 °C): 81.5.

[Pd(η^3 -CH₂CMeCH₂)(ON-*i*Pr)]SbF₆ (11). This complex was prepared analogously to complex 6a using 5b (196 mg, 0.50 mmol), 2a (237 mg, 1.05 mmol), and AgSbF₆ (343 mg, 1.00 mmol) as starting materials. Yield: 556 mg (89%). Anal. Calcd for $C_{15}H_{26}F_6N_2OPPdSb$: C, 28.90; H, 4.20; N, 4.49. Found: C, 28.95; H, 4.29; N, 4.59. 1H NMR (δ , CD_2Cl_2 , 20 °C): 8.24 (d, $J = 5.3$ Hz, 1H, py^6), 7.86 (t, $J = 7.5$ Hz, 1H, py^3), 7.30 (d, $J = 8.3$ Hz, 1H, py^4), 7.08 (t, $J = 6.4$ Hz, 1H, py^5), 6.26

(d, $J = 12.0$ Hz, 1H, NH), 3.97 (s, 1H_{av}, CH), 3.63 (s, 1H_{av}, CH), 3.13 (s, 1H_{av}, CH), 2.92 (s, 1H_{av}, CH), 2.37 (s, $J = 6.3$ Hz, 2H, CH), 2.23 (s, 3H, CH₃), 1.4–1.02 (m, 12H, CH₃). $^{13}\text{C}\{^1\text{H}\}$ NMR (δ , CD₂Cl₂, 20 °C): 155.6 (s, py²), 152.1 (s, py⁶), 141.2 (s, py⁴), 132.8 (s, CCH₃), 119.4 (s, py³), 118.6 (s, py⁵), 61.5 (s, CH₂), 57.9 (s, CH₂), 26.4 (d, $J_{\text{CP}} = 89.6$ Hz, CH), 22.8 (s, CH₃), 15.1 (d, $J_{\text{CP}} = 3.4$ Hz, CH₃), 14.7 (s, CH₃). $^{31}\text{P}\{^1\text{H}\}$ NMR (δ , CD₂Cl₂, 20 °C): 81.3.

[Pd(η^3 -CHPhCHCH₂)(ON-Ph)]SbF₆ (12a). This complex was prepared analogously to complex **6a** using **5d** (129 mg, 0.25 mmol), **2a** (158 mg, 0.54 mmol), and AgSbF₆ (172 mg, 0.50 mmol) as starting materials. Yield: 372 mg (98%). Anal. Calcd for C₂₆H₂₄F₆N₂OPdSb: C, 41.44; H, 3.21; N, 3.72. Found: C, 41.52; H, 3.16; N, 3.60. ^1H NMR (δ , CD₂Cl₂, 20 °C): 8.14 (d, $J = 6.1$ Hz, 1H, py⁶), 7.94 (t, $J = 7.8$ Hz, 1H, py³), 7.86–7.42 (m, 15H, Ph, py), 7.34 (dd, $J = 16.0, 7.9$ Hz, 2H, NH, Ph), 7.22 (t, $J = 6.7$ Hz, 1H, py⁴), 6.25–6.0 (m, 1H_c), 4.77 (d, $J = 11.1$ Hz, 1H_a), 4.17 (d, $J = 5.6$ Hz, 1H_s), 3.22 (d, $J = 11.8$ Hz, 1H_a). $^{13}\text{C}\{^1\text{H}\}$ NMR (δ , CD₂Cl₂, 20 °C): 152.4 (s, py²), 148.6 (s, py⁶), 143.3 (s, py⁴), 135.6 (s, Ph), 132.0 (d, $J_{\text{CP}} = 11.6$ Hz, Ph), 129.8 (d, $J_{\text{CP}} = 14.1$ Hz, Ph), 128.2 (s, Ph), 124. Eight (s, Ph), 122.7 (s, Ph), 120.9 (s, CH), 118.5 (s, py³), 108.0 (s, py⁵), 80.7 (s, CH₂), 67.5 (s, CH₂). $^{31}\text{P}\{^1\text{H}\}$ NMR (δ , CD₂Cl₂, 20 °C): 58.3.

[Pd(η^3 -CHPhCHCH₂)(ON-*i*Pr)]SbF₆ (12b). This complex was prepared analogously to complex **6a** using **5d** (129 mg, 0.25 mmol), **2a** (120 mg, 0.54 mmol), and AgSbF₆ (172 mg, 0.50 mmol) as starting materials. Yield: 329 mg (96%). Anal. Calcd for C₂₀H₂₈F₆N₂OPdSb: C, 35.04; H, 4.12; N, 4.09. Found: C, 35.20; H, 4.14; N, 3.98. ^1H NMR (δ , CD₂Cl₂, 20 °C): 8.26 (s, 1H, py⁶), 7.81 (s, 1H, py³), 7.67–6.82 (m, 7H, Ph, py^{4,5}), 6.44 (d, $J = 9.3$ Hz, 1H, NH), 6.28–6.08 (m, 1H, CH), 5.20–3.50 (m, 2H, CH₂), 3.21 (s, 1H, CH), 2.65–1.80 (m, 2H, CH), 1.48–0.46 (m, 12H, CH₃). $^{13}\text{C}\{^1\text{H}\}$ NMR (δ , CD₂Cl₂, 20 °C): 155.5 (s, py²), 152.3 (s, py⁶), 141.1 (s, py⁴), 136.2 (s, Ph), 129.2 (s, Ph), 128.8 (s, Ph), 127.9 (s, Ph), 119.3 (s, CH), 118.5 (s, py⁵), 109.4 (py³), 81.1 (s, CH), 56.0 (s, CH₂), 26.5 (d, $J_{\text{CP}} = 110.7$ Hz, CH), 15.3 (s, CH₃), 14.7 (s, CH₃). $^{31}\text{P}\{^1\text{H}\}$ NMR (δ , CD₂Cl₂, 20 °C): 81.3.

[Pd(η^3 -CHPhCHCHPh)(ON-*i*Pr)]SbF₆ (13). This complex was prepared analogously to complex **6a** using **5e** (167 mg, 0.25 mmol), **2b** (120 mg, 0.54 mmol), and AgSbF₆ (172 mg, 0.50 mmol) as starting materials. Yield: 350 mg (92%). Anal. Calcd for C₂₆H₃₂F₆N₂OPdSb: C, 41.00; H, 4.23; N, 3.68. Found: C, 40.97; H, 4.13; N, 3.72. ^1H NMR (δ , CD₂Cl₂, 20 °C): 7.87–7.20 (m, 13H, Ph, NH, py), 7.11 (d, $J = 8.2$ Hz, 1H, py⁵), 6.64–6.37 (m, 2H, py⁵, CH), 6.28 (d, $J = 10.8$ Hz, CH), 4.83 (bs, 1H, CH), 2.38–1.96 (m, 2H, CH), 1.11 (d, 14.7 Hz, 6H, CH₃), 0.86 (d, $J = 11.5$ Hz, 6H, CH₃). $^{13}\text{C}\{^1\text{H}\}$ NMR (δ , CD₂Cl₂, 20 °C): 155.2 (d, $J_{\text{CP}} = 4.8$ Hz, py²), 150.2 (s, py⁶), 140.6 (s, py⁴), 136.8 (s, Ph), 131.0–129.2 (Ph), 128.9 (s, Ph), 128.1 (s, Ph), 119.1 (s, py⁵), 117.7 (s, CH), 117.6 (s, py³), 103.8 (s, Ph), 78.9 (s, CH), 73.8 (s, CH), 26.4 (d, $J_{\text{CP}} = 82.6$ Hz, CH), 15.0 (d, $J_{\text{CP}} = 36.9$ Hz, CH₃), 14.3 (d, $J_{\text{CP}} = 40.0$ Hz, CH₃). $^{31}\text{P}\{^1\text{H}\}$ NMR (δ , CD₂Cl₂, 20 °C): 80.9.

[Pd(η^3 -CH₂CHCH₂)(SN-Ph)]SbF₆ (14a). This complex was prepared analogously to complex **6a** using **5a** (184 mg, 0.50 mmol), **3a** (330 mg, 1.06 mmol), and AgSbF₆ (343 mg, 1.00 mmol) as starting materials. Yield: 622 mg (90%). Anal. Calcd for C₂₀H₂₀F₆N₂SPPdSb: C, 34.64; H, 2.91; N, 4.04. Found: C, 34.55; H, 2.89; N, 4.12. ^1H NMR (δ , CD₂Cl₂, 20 °C): 8.28 (d, $J = 5.7$ Hz, 1H, py⁶), 7.96–7.77 (m, 5H, py⁴, Ph), 7.77–7.66 (m, 2H, Ph), 7.66–7.50 (m, 4H, Ph), 7.27 (d, $J = 8.4$ Hz, 1H, py³), 7.05 (t, $J = 7.1$ Hz, 1H, py⁵), 6.93 (d, $J = 5.3$ Hz, 1H, NH), 5.09 (m, 1H, CH), 4.25 (bs, 1H_s, CH), 3.91 (bs, 1H_s, CH), 3.25 (bd, $J = 11.8$ Hz, 1H_a, CH), 2.72 (bd, $J = 10.6$ Hz, 1H_a, CH). $^{13}\text{C}\{^1\text{H}\}$ NMR (δ , CD₂Cl₂, 20 °C): 153.8 (d, $J = 4.0$ Hz, py²), 152.3 (s, py⁶), 141.1 (s, py⁴), 134.0 (s, Ph), 131.2 (d, $J_{\text{CP}} = 12.5$ Hz, Ph), 129.5 (d, $J_{\text{CP}} = 14.2$ Hz, Ph), 119.1 (s, CH), 117.8 (d, $J_{\text{CP}} = 6.8$ Hz, py³), 117.6 (s, py⁵), 75.0 (s, CH₂), 59.7 (s, CH₂). $^{31}\text{P}\{^1\text{H}\}$ NMR (δ , CD₂Cl₂, 20 °C): 60.9.

[Pd(η^3 -CH₂CHCH₂)(SN-*i*Pr)]SbF₆ (14b). This complex was prepared analogously to complex **6a** using **5a** (366 mg, 1.00 mmol), **3b**

(500 mg, 2.06 mmol), and AgSbF₆ (686 mg, 2.00 mmol) as starting materials. Yield: 1.1 g (88%). Anal. Calcd for C₁₄H₂₄F₆N₂SPPdSb: C, 26.88; H, 3.87; N, 4.48. Found: C, 26.75; H, 3.97; N, 4.50. ^1H NMR (δ , CD₂Cl₂, 20 °C): 8.37 (dd, $J = 5.7, 1.7$ Hz, 1H, py⁶), 7.86 (dd, $J = 8.3, 1.8$ Hz, 1H, py³), 7.37 (d, $J = 8.4$ Hz, 1H, py⁴), 7.11 (t, $J = 6.5$ Hz, 1H, py⁵), 6.38 (dd, $J = 7.0, 0.7$ Hz, 1H, NH), 5.86–5.60 (m, 1H_c, CH), 4.42 (d, $J = 5.2$ Hz, 1H_s, CH), 4.07 (d, $J = 6.8$ Hz, 1H_s, CH), 3.54 (d, $J = 12.6$ Hz, 1H_{av}, CH), 3.07 (d, $J = 12.3$ Hz, 1H_{av}, CH), 2.77–2.49 (m, 2H, CH), 1.48–1.12 (m, 12H, CH₃). $^{13}\text{C}\{^1\text{H}\}$ NMR (δ , CD₂Cl₂, 20 °C): 154.1 (d, $J = 5.7$ Hz, py²), 152.1 (s, py⁶), 141.1 (s, py⁴), 119.9 (s, CH), 119.8 (s, py³), 117.1 (s, py⁵), 73.4 (s, CH₂), 58.1 (s, CH₂), 30.3 (d, $J_{\text{CP}} = 54.9$ Hz, CH), 6.0 (d, $J_{\text{CP}} = 3.5$ Hz, CH₃). $^{31}\text{P}\{^1\text{H}\}$ NMR (δ , CD₂Cl₂, 20 °C): 100.0. The same complex with CF₃SO₃[−] as counterion was obtained by using AgCF₃SO₃ as halide scavenger.

[Pd(η^3 -CH₂CMeCH₂)(SN-Ph)]SbF₆ (15a). This complex was prepared analogously to complex **6a** using **5b** (196 mg, 0.50 mmol), **3a** (330 mg, 1.06 mmol), and AgSbF₆ (343 mg, 1.00 mmol) as starting materials. Yield: 630 mg (89%). Anal. Calcd for C₂₁H₂₂F₆N₂SPPdSb: C, 35.65; H, 3.13; N, 3.96. Found: C, 35.59; H, 3.17; N, 4.01. ^1H NMR (δ , CD₂Cl₂, 20 °C): 9.06 (s, 1H, NH), 8.59 (d, $J = 4.7$ Hz, 1H, py⁶), 8.33–7.50 (m, 11H, py³, Ph), 7.42 (d, $J = 8.7$ Hz, 1H, py⁴), 7.16 (t, $J = 5.8$ Hz, 1H, py⁵), 4.31 (s, 1H_{av}, CH), 3.82 (s, 1H_{av}, CH), 3.44 (s, 1H_{av}, CH), 2.85 (s, 1H_{av}, CH), 1.65 (s, 3H, CH₃). $^{13}\text{C}\{^1\text{H}\}$ NMR (δ , CD₂Cl₂, 20 °C): 153.7 (d, $J = 3.0$ Hz, py²), 152.5 (s, py⁶), 141.0 (s, py⁴), 134.7 (s, CCH₃), 133.9 (s, Ph), 131.1 (d, $J_{\text{CP}} = 12.0$ Hz, Ph), 129.6 (s, Ph), 119.0 (s, py³), 117.7 (d, $J_{\text{CP}} = 5.7$ Hz, py⁵), 73.8 (s, CH₂), 58.7 (s, CH₂), 21.9 (s, CH₃). $^{31}\text{P}\{^1\text{H}\}$ NMR (δ , CD₂Cl₂, 20 °C): 59.7.

[Pd(η^3 -CH₂CMeCH₂)(SN-*i*Pr)]SbF₆ (15b). This complex was prepared analogously to complex **6a** using **5b** (196 mg, 0.50 mmol), **3b** (240 mg, 1.07 mmol), and AgSbF₆ (343 mg, 1.00 mmol) as starting materials. Yield: 607 mg (95%). Anal. Calcd for C₁₅H₂₆F₆N₂SPPdSb: C, 28.17; H, 4.10; N, 4.38. Found: C, 28.19; H, 4.02; N, 4.48. ^1H NMR (δ , CD₂Cl₂, 20 °C): 8.38 (d, $J = 4.9$ Hz, 1H, py⁶), 7.86 (t, $J = 7.5$ Hz, 1H, py³), 7.35 (d, $J = 8.3$ Hz, 1H, py⁴), 7.10 (t, $J = 6.3$ Hz, 1H, py⁵), 6.34 (d, $J = 6.9$ Hz, 1H, NH), 4.20 (s, 1H_{av}, CH), 3.85 (s, 1H_s, CH₂), 3.38 (s, 1H_{av}, CH), 2.97 (s, 1H_{av}, CH₂), 2.78–2.46 (m, 2H, CH), 2.14 (s, 3H, CH₃), 1.47–1.13 (m, 12H, CH₃). $^{13}\text{C}\{^1\text{H}\}$ NMR (δ , CD₂Cl₂, 20 °C): 154.1 (d, $J = 5.0$ Hz, py²), 152.2 (s, py⁶), 141.1 (s, py⁴), 133.7 (s, CCH₃), 119.8 (d, $J_{\text{CP}} = 4.5$ Hz, py³), 119.7 (s, py⁵), 71.9 (s, CH₂), 57.7 (s, CH₂), 30.4 (d, $J_{\text{CP}} = 57.1$ Hz, CH), 23.0 (s, CH₃), 15.8 (d, $J_{\text{CP}} = 24.2$ Hz, CH₃). $^{31}\text{P}\{^1\text{H}\}$ NMR (δ , CD₂Cl₂, 20 °C): 99.8.

[Pd(η^3 -CHPhCHCH₂)(SN-Ph)]SbF₆ (16a). This complex was prepared analogously to complex **6a** using **5d** (129 mg, 0.25 mmol), **3a** (165 mg, 0.53 mmol), and AgSbF₆ (172 mg, 0.50 mmol) as starting materials. Yield: 362 mg (98%). Anal. Calcd for C₂₆H₂₄F₆N₂SPPdSb: C, 40.57; H, 3.14; N, 3.64. Found: C, 40.62; H, 3.18; N, 3.50. ^1H NMR (δ , CD₂Cl₂, 20 °C): 8.03–7.80 (m, 9H, py⁶, Ph), 7.80–7.59 (m, 9H, py³, Ph), 7.33 (d, $J = 18.0$ Hz, 2H, Ph), 7.18 (d, $J = 3.1$ Hz, 1H, py⁴), 7.07 (s, 1H, NH), 7.03–6.80 (m, 1H, py⁵), 6.62 (bs, 1H_c, CH), 5.51 (bs, 1H_s, CH), 4.61 (d, $J = 11.5$ Hz, 1H_{av}, CH), 3.92 (d, $J = 3.6$ Hz, 1H_{av}, CH). $^{13}\text{C}\{^1\text{H}\}$ NMR (δ , CD₂Cl₂, 20 °C): 149.9 (s, py²), 140.5 (s, py⁶), 134.0 (d, $J_{\text{CP}} = 2.9$ Hz, py⁴), 131.2 (d, $J_{\text{CP}} = 12.5$ Hz, Ph), 130.14–129.02 (Ph), 127.81 (s, Ph), 119.0 (s, CH), 116.5 (d, $J_{\text{CP}} = 6.8$ Hz, py³), 110.37 (s, py⁵), 92.6 (s, CH), 57.33 (s, CH₂). $^{31}\text{P}\{^1\text{H}\}$ NMR (δ , CD₂Cl₂, 20 °C): 60.0.

[Pd(η^3 -CHPhCHCH₂)(SN-*i*Pr)]SbF₆ (16b). This complex was prepared analogously to complex **6a** using **5d** (129 mg, 0.25 mmol), **3b** (125 mg, 0.52 mmol), and AgSbF₆ (172 mg, 0.50 mmol) as starting materials. Yield: 334 mg (95%). Anal. Calcd for C₂₀H₂₈F₆N₂PPdSb: C, 34.24; H, 4.02; N, 3.99. Found: C, 34.10; H, 4.14; N, 3.98. ^1H NMR (δ , CD₂Cl₂, 20 °C): 7.78–7.15 (m, 8H, py, Ph), 6.97 (d, $J = 6.9$ Hz, 1H, py³), 6.62 (s, 1H, NH), 6.16 (bs, 1H_c, CH), 5.00 (d, $J = 11.1$ Hz, 1H_{av}, CH), 4.08 (bs, 1H_{av}, CH), 3.11 (bs, 1H_{av}, CH), 2.59 (s, 2H, CH), 1.65–0.89 (m, 12H, CH₃). $^{13}\text{C}\{^1\text{H}\}$ NMR (δ , CD₂Cl₂, 20 °C):

153.9 (s, py²), 149.7 (s, py⁶), 140.3 (s, py⁴), 129.5 (s, Ph), 129.0 (s, Ph), 127.7 (s, Ph), 119.7 (s, CH), 118.8 (s, py³), 109.8 (s, py²), 90.6 (s, CH), 55.4 (s, CH₂), 30.7 (d, $J_{CP} = 44.6$ Hz, CH), 29.8 (d, $J_{CP} = 41.8$ Hz, CH), 16.1 (s, CH₃). ³¹P{¹H} NMR (δ, CD₂Cl₂, 20 °C): 99.5.

[Pd(η³-CH₂CHCH₂)(SeN-Ph)]SbF₆ (17a). This complex was prepared analogously to complex 6a using 5a (184 mg, 0.50 mmol), 4a (390 mg, 1.09 mmol), and AgSbF₆ (343 mg, 1.00 mmol) as starting materials. Yield: 629 mg (85%). Anal. Calcd for C₂₀H₂₀F₆N₂PPdSbSe: C, 32.44; H, 2.72; N, 3.78. Found: C, 32.53; H, 2.68; N, 3.81. ¹H NMR (δ, CD₂Cl₂, 20 °C): 8.32 (d, $J = 5.6$ Hz, 1H, py⁶), 7.94–7.78 (m, py³, Ph), 7.77–7.48 (m, 6H, py⁴, Ph), 7.26 (d, $J = 8.4$ Hz, 1H, py⁵), 7.06 (t, $J = 6.6$ Hz, 1H, py), 6.92 (s, $J = 6.30$ Hz, 1H, NH), 5.01–4.81 (m, 1H, CH), 4.34 (s, 1H_s, CH₂), 3.88 (s, 1H_s, CH₂), 3.21 (s, 1H_a, CH₂), 2.52 (s, 1H_a, CH₂). ¹³C{¹H} NMR (δ, CD₂Cl₂, 20 °C): 153.9 (d, $J_{CP} = 19.1$ Hz, py²), 151.8 (s, py⁶), 144.6 (s, py⁴), 140.9 (s, Ph), 133.9 (s, Ph), 131.1 (d, $J_{CP} = 12.8$ Hz, Ph), 129.4 (d, $J_{CP} = 14.2$ Hz, Ph), 119.0 (s, CH), 117.8 (d, $J_{CP} = 6.7$ Hz, py³), 116.7 (s, py⁵), 76.4 (s, CH₂), 57.9 (s, CH₂). ³¹P{¹H} NMR (δ, CD₂Cl₂, 20 °C): 50.3 (d, $J_{P-Se} = 651.2$ Hz).

[Pd(η³-CH₂CHCH₂)(SeN-*i*Pr)]SbF₆ (17b). This complex was prepared analogously to complex 6a using 5a (184 mg, 0.50 mmol), 4a (3.05 mg, 1.05 mmol), and AgSbF₆ (343 mg, 1.00 mmol) as starting materials. Yield: 578 mg (86%). Anal. Calcd for C₁₄H₂₄F₆N₂PPdSbSe: C, 25.01; H, 3.60; N, 4.17. Found: C, 25.15; H, 3.49; N, 4.20. ¹H NMR (δ, CD₂Cl₂, 20 °C): 8.66 (d, $J = 3.6$ Hz, 1H, py⁶), 8.44 (s, 1H, NH), 7.97 (t, $J = 7.7$ Hz, 1H, py³), 7.53 (d, $J = 7.7$ Hz, 1H, py⁴), 7.20 (t, $J = 5.1$ Hz, 1H, py⁵), 5.96–5.73 (m, 1H, CH), 4.62 (bs, 1H_s, CH), 4.12 (bs, 1H_s, CH), 3.75 (bs, 1H_a, CH), 3.09 (bs, 1H_a, CH), 2.98–2.68 (m, 2H, CH), 1.45–1.14 (m, 12H, CH₃). ¹³C{¹H} NMR (δ, CD₂Cl₂, 20 °C): 155.2 (d, $J_{CP} = 6.04$ Hz, py²), 151.6 (s, py⁶), 140.5 (s, py⁴), 120.5 (d, $J_{CP} = 4.4$ Hz, CH), 119.2 (s, py³), 116.0 (s, py⁵), 74.8 (s, CH₂), 55.4 (s, CH₂), 30.6 (d, $J_{CP} = 46.4$ Hz, CH), 16.6 (d, $J_{CP} = 3.2$ Hz, CH₃). ³¹P{¹H} NMR (δ, CD₂Cl₂, 20 °C): 94.5 (d, $J_{P-Se} = 634.8$ Hz). The same complex with CF₃SO₃⁻ as counterion was obtained by using AgCF₃SO₃ as halide scavenger.

[Pd(η³-CH₂CMeCH₂)(κ¹(N)-ON-Ph)Cl] (18). A mixture of 5b (100 mg, 0.25 mmol) and 2a (160 mg, 0.54 mmol) in CH₂Cl₂ (10 mL) was stirred for 30 min. After that, the solvent was removed under reduced pressure. The remaining solid was washed with diethyl ether and dried under vacuum. Yield: 246 mg (100%). Anal. Calcd for C₂₁H₂₂ClN₂OOPd: C, 51.35; H, 4.51; N, 5.70. Found: C, 51.39; H, 4.59; N, 5.68. ¹H NMR (δ, CD₂Cl₂, 20 °C): 8.28 (d, $J = 4.6$ Hz, 1H py⁶), 8.05–7.89 (m, 4H, py, Ph), 7.70–7.40 (m, 7H, py, Ph), 7.27 (d, $J = 8.3$ Hz, 1H, py⁴), 6.87 (t, $J = 5.9$ Hz, 1H, py⁵), 5.35 (s, 1H, NH), 3.79 (s, 2H, CH₂), 2.91 (s, 2H, CH₂), 2.05 (s, 3H, CH₃). ¹³C{¹H} NMR (δ, CD₂Cl₂, 20 °C): 154.7 (s, py), 150.6 (s, py), 139.0 (s, py), 132.4 (d, $J_{CP} = 2.8$ Hz, py), 131.7 (d, $J_{CP} = 10.5$ Hz, Ph), 130.3 (d, $J_{CP} = 23.3$ Hz, Ph), 128.8 (d, $J_{CP} = 13.2$ Hz, Ph), 117.3 (s, CH), 114.2 (s, Ph), 61.5 (s, CH₂), 55.3 (s, CH₂), 22.8 (s, CH₃). ³¹P{¹H} NMR (δ, CD₂Cl₂, 20 °C): 31.7.

[Pd(η³-CH₂CHCH₂)(SN^H-*i*Pr)] (19). A solution of 14b (191 mg, 0.30 mmol) in THF (10 mL) was cooled to 0 °C using an ice bath. Then, KO^tBu (34 mg, 0.30 mmol) dissolved in THF was added dropwise to this solution, and the mixture was allowed to stir for 30 min. After that, the solvent was evaporated under reduced pressure. The solid was dissolved in benzene, the remaining potassium salt was filtered off, and the solvent was removed under vacuum to give analytically pure 25. Yield: 116 mg (99%). Anal. Calcd for C₁₄H₂₃N₂PPdS: C, 43.25; H, 5.96; N, 7.21. Found: C, 43.30; H, 5.88; N, 7.32. ¹H NMR (δ, C₆D₆, 20 °C): 7.99 (d, $J = 5.1$ Hz, 1H, py⁶), 7.27 (t, $J = 7.6$ Hz, 1H, py³), 6.66 (d, $J = 8.5$ Hz, 1H, py⁴), 6.27 (t, $J = 6.0$ Hz, 1H, py⁵), 5.64–5.43 (m, 1H, CH), 4.01 (d, $J = 6.4$ Hz, 1H_s, CH₂), 3.65 (d, $J = 6.5$ Hz, 1H_s, CH₂), 3.30 (d, $J = 12.5$ Hz, 1H_a, CH₂), 2.75 (d, $J = 12.3$ Hz, 1H_a, CH₂), 2.33–2.05 (m, 2H, CH), 1.36–1.02 (m, 12H, CH₃). ¹³C{¹H} NMR (δ, C₆D₆, 20 °C): 164.6 (s, py²), 152.5 (s, py⁶), 136.7 (d, $J_{CP} = 3.2$ Hz, py⁴), 122.7 (d, $J_{CP} = 18.3$ Hz,

py⁵), 113.6 (s, CH), 109.8 (s, py³), 70.6 (s, CH₂), 53.0 (s, CH₂), 31.0 (d, $J_{CP} = 14.9$ Hz, CH), 29.8 (d, $J_{CP} = 16.0$ Hz, CH), 16.6 (s, CH₃). ³¹P{¹H} NMR (δ, C₆D₆, 20 °C): 64.2.

X-ray Structure Determination. X-ray data for (ON-Ph) (2a), (ON-*i*Pr) (2b), [Pd(η³-CH₂CMeCH₂)(PN-*i*Pr)]SbF₆ (7b), [Pd(η³-CHPhCHCH₂)(PN-*i*Pr)]SbF₆ (8b), [Pd(η³-CHPhCHCHPh)(PN-*i*Pr)]SbF₆ (9), [Pd(η³-CH₂CHCH₂)(ON-*i*Pr)]SbF₆ (10), [Pd(η³-CH₂CHCH₂)(SN-*i*Pr)]CF₃SO₃ (14b), [Pd(η³-CH₂CMeCH₂)(SN-Ph)]SbF₆ (15a), [Pd(η³-CH₂CMeCH₂)(SN-*i*Pr)]SbF₆ (15b), [Pd(η³-CH₂CHCH₂)(SeN-*i*Pr)]CF₃SO₃ (17b), [Pd(η³-CH₂CMeCH₂)(κ¹(N)-ON-Ph)Cl] · 1/2CH₂Cl₂ (18 · 1/2CH₂Cl₂), and [Pd(η³-CH₂CHCH₂)(SN^H-*i*Pr)] (19) were collected at $T = 100$ K on a Bruker Kappa APEX-2 CCD area detector diffractometer using graphite-monochromated Mo $K\alpha$ radiation ($\lambda = 0.71073$ Å) and φ - and ω -scan frames covering complete spheres of the reciprocal space with $\theta_{\max} = 30^\circ$. Corrections for absorption and $\lambda/2$ effects were applied.⁴³ After structure solution with the program SHELXS97 and direct methods, refinement on F^2 was carried out with the program SHELXL97.⁴⁴ Non-hydrogen atoms were refined anisotropically. Most hydrogen atoms were placed in calculated positions and thereafter treated as riding. The allyl groups in 10, 14b, 17b, and 19 showed orientation disorder with the central allyl carbon atom adopting two complementary positions (up and down orientation of the allyl group relative to the Pd coordination plane). This feature was taken into account in the refinement. All substituted allyl groups were ordered. Allyl group hydrogen atoms were handled with instructions AFIX 23 for CH₂ and AFIX 43 for CH. The two triflate salts 14b and 17b, [Pd(η³-CH₂CHCH₂)(EN-*i*Pr)]CF₃SO₃ with E = S or Se, are isostructural. Compound 18 crystallized as a stable stoichiometric dichloromethane solvate (2:1) with two independent Pd complexes differing in conformation and one solvent molecule. All complexes except 18 · 1/2CH₂Cl₂ and 19 showed intermolecular hydrogen bonds between the N–H group of the chelate ligand and the counteranion. In 19 the deprotonated nitrogen atom N2 is an acceptor of a weak C–H ··· N interaction from CH of a isopropyl group, C ··· N = 3.57 Å. Crystallographic data are listed in Table S2. Selected geometric data are given in Table S1.

Computational Details. All calculations were performed using the Gaussian 03 software package⁴⁵ and the PBE0 functional, without symmetry constraints. That functional uses a hybrid generalized gradient approximation, including a 25% mixture of Hartree–Fock⁴⁶ exchange with DFT³⁵ exchange–correlation, given by the Perdew, Burke, and Ernzerhof functional (PBE).⁴⁷ The optimized geometries were obtained with a LanL2DZ basis set⁴⁸ augmented with an f-polarization function⁴⁹ for Pd and a standard 6-31G(d,p)⁵⁰ for the remaining elements (basis b1). Transition-state optimizations were performed with the synchronous transit-guided quasi-Newton method (STQN) developed by Schlegel et al.,⁵¹ following extensive searches of the potential energy surface. Frequency calculations were performed to confirm the nature of the stationary points, yielding one imaginary frequency for the transition states and none for the minima. Each transition state was further confirmed by following its vibrational mode downhill on both sides and obtaining the minima presented on the energy profiles. A natural population analysis⁵² and the resulting Wiberg indices³⁶ were used to study the electronic structure and bonding of the optimized species.

The energy profiles reported result from single-point energy calculations using an improved basis set (basis b2) and the geometries optimized at the PBE0/b1 level. Basis b2 consisted of the Stuttgart/Dresden ECP basis set⁵³ with an added f-polarization function⁴⁹ for Pd and standard 6-311++G(d,p)⁵⁴ for the remaining elements. Solvent effects (CH₃CN) were considered in the PBE0/b2//PBE0/b1 energy calculations using the polarizable continuum model initially devised by Tomasi and co-workers⁵⁵ as implemented in Gaussian 03.⁵⁶ The molecular cavity was based on the united atom topological model applied on UAHF radii, optimized for the HF/6-31G(d) level.

Suzuki–Miyaura Cross-Coupling Reactions. General Procedure. In a glovebox, a vial equipped with a magnetic stir bar was charged with a solution of phenylboronic acid (1.5 mmol), aryl bromide (1 mmol), and KOtBu (2 mmol) in 2-propanol (5 mL, HPLC grade), and the required amount of palladium catalyst solution (prepared from a 0.01 M solution of the catalyst in CH₂Cl₂) was added by syringe. The reaction mixture was stirred at room temperature unless otherwise indicated. After 12 h the reaction was quenched with a saturated NaHCO₃ solution. The product was then extracted with diethyl ether (3 × 5 mL). The combined organic layers were washed with brine, dried over Na₂SO₄, and filtered, and the solvent was evaporated under vacuum. When necessary the product was purified by flash chromatography on silica gel.

■ ASSOCIATED CONTENT

Supporting Information. Complete crystallographic data and technical details in CIF format and tabular form for compounds **2a**, **2b**, **7b**, **8b**, **9**, **10**, **14b**, **15a**, **15b**, **17b**, **18** · 1/2CH₂Cl₂, and **19**. Molecular structures of **2a** and **2b** (Figures S1 and S2). Energy profiles for η^3 -allyl pseudorotation in **6b**⁺ (Figure S3) and η^2 - η^1 - η^3 allyl isomerization in **14b**⁺ (Figure S4). Atomic coordinates for all optimized species. This material is available free of charge via the Internet at <http://pubs.acs.org>.

■ AUTHOR INFORMATION

Present Addresses

¹Visiting Professor at the Institute of Applied Synthetic Chemistry (Sept 2010–Aug 2011).

■ ACKNOWLEDGMENT

L.F.V. acknowledges UTL/Santander and Fundação para a Ciência e Tecnologia (FCT, project PEst-OE/QUI/UI0100/2011) for financial support.

■ REFERENCES

- (1) (a) Bader, A.; Lindner, E. *Coord. Chem. Rev.* **1991**, *108*, 27–110, and references therein. (b) Bassetti, M. *Eur. J. Inorg. Chem.* **2006**, 4473–4482. (c) Helmchen, G.; Pfaltz, A. *Acc. Chem. Res.* **2000**, *33*, 336–345. (d) McManus, H. A.; Guiry, P. *Chem. Rev.* **2004**, *104*, 4151–4202. (e) Braunstein, P. *Chem. Rev.* **2006**, *106*, 134–159. (f) Grushin, V. V. *Chem. Rev.* **2004**, *104*, 1629–1662. (g) Ly, T. Q.; Woollins, J. D. *Coord. Chem. Rev.* **1998**, *176*, 451–481.
- (2) Benito-Garagorri, D.; Mereiter, K.; Kirchner, K. *Collect. Czech. Chem. Commun.* **2007**, *72*, 527–540.
- (3) (a) Standfest-Hauser, C. M.; Dazinger, G.; Wiedermann, J.; Mereiter, K.; Kirchner, K. *Eur. J. Inorg. Chem.* **2009**, 4085–4093. (b) Lackner-Warton, W.; Tanaka, S.; Standfest-Hauser, C. M.; Öztöpcü, Ö.; Hsieh, J.-C.; Mereiter, K.; Kirchner, K. *Polyhedron* **2010**, *29*, 3097–3102.
- (4) Zhao, W.-J.; Zhang, S.-J.; Deng, Y.; Zhang, Z.-Z.; Ma, Y.-F.; Huang, W.-P.; Wang, H.-G. *Jiegou Huaxue* **1996**, *15*, 44–46.
- (5) Seidel, W.; Schöler, H. Z. *Chem.* **1967**, *11*, 431.
- (6) Ainscough, W.; Peterson, L. K. *Inorg. Chem.* **1970**, *9*, 2699–2705.
- (7) Brunner, H.; Weber, H. *Chem. Ber.* **1985**, *118*, 3380–3395.
- (8) (a) Schirmer, W.; Flörke, U.; Haupt, H. J. Z. *Anorg. Allg. Chem.* **1987**, *545*, 83–97. (b) Schirmer, W.; Flörke, U.; Haupt, H. J. Z. *Anorg. Allg. Chem.* **1989**, *574*, 239–255.
- (9) Aucott, S. M.; Slawin, A. M. Z.; Woollins, J. D. *Phosphorus, Sulfur, Silicon* **1997**, *124–125*, 473–476.
- (10) (a) Aucott, S. M.; Slawin, A. M. Z.; Woollins, J. D. *J. Chem. Soc., Dalton Trans.* **2000**, 2559–2575. (b) Clarke, M. L.; Slawin, A. M. Z.; Wheatley, M. V.; Woollins, J. D. *J. Chem. Soc., Dalton Trans.* **2001**, 3421–3429. (c) Slawin, A. M. Z.; Wheatley, J.; Wheatley, M. V.; Woollins, J. D. *Polyhedron* **2003**, *22*, 1397–1405.
- (11) Sanchez, G.; Garcia, J.; Meseguer, D.; Serrano, J. L.; Garcia, L.; Perez, J.; Lopez, G. *Inorg. Chim. Acta* **2004**, *357*, 4568–4576.
- (12) (a) Smolensky, E.; Kapon, M.; Woollins, J. D.; Eisen, M. S. *Organometallics* **2005**, *24*, 3255–3265. (b) Smolensky, E.; Kapon, M.; Eisen, M. S. *Organometallics* **2007**, *26*, 4510–4527.
- (13) Nabavizadeh, S. M.; Tabei, E. S.; Hosseini, F. N.; Keshavarz, N.; Jamali, S.; Rashidi, M. *New J. Chem.* **2010**, *34*, 495–499.
- (14) (a) Hyder, I.; Jimenez-Tenorio, M.; Puerta, M. C.; Valerga, P. *Organometallics* **2011**, *30*, 726–737. (b) Macias-Arce, I.; Puerta, M. C.; Valerga, P. *Eur. J. Inorg. Chem.* **2010**, 1767–1776.
- (15) Henning, H.-G.; Ladhoff, U. Z. *Chem.* **1973**, *13*, 16–17.
- (16) For related tridentate ENE ligands see for example: Biricik, N.; Fei, Z.; Scopelliti, R.; Dyson, P. J. *Helv. Chim. Acta* **2003**, *86*, 3281–3287.
- (17) (a) Trost, B. M.; Verhoeven, T. R. In *Comprehensive Organometallic Chemistry*; Wilkinson, G.; Stone, F. G. A.; Abel, E. W., Eds.; Pergamon Press: Oxford, 1982; Vol. 8, p 799. (b) von Matt, P.; A. Pfaltz, A. *Angew. Chem., Int. Ed. Engl.* **1993**, *32*, 566–568. (c) Hayashi, T. In *Catalytic Asymmetric Synthesis*; Ojima, I., Ed.; VCH Publishers: New York, 1993; p 325, and references therein. (d) Noyori, R. *Asymmetric Catalysis in Organic Synthesis*; Wiley: New York, 1994; p 82. (e) Trost, B. M.; Vranken, D. L. V. *Chem. Rev.* **1996**, *96*, 395–422. (f) Consiglio, G.; Waymouth, R. M. *Chem. Rev.* **1989**, *89*, 257–276. (g) Frost, C. G.; Howarth, J.; Williams, J. M. J. *Tetrahedron: Asymmetry* **1992**, *3*, 1089–1122. (h) Helmchen, G. *J. Organomet. Chem.* **1999**, *576*, 203–214.
- (18) Benito-Garagorri, D.; Mereiter, K.; Kirchner, K. *Collect. Czech. Chem. Commun.* **2007**, *72*, 527–540.
- (19) Vrieze, K. Fluxional Allyl Complexes. In *Dynamic Nuclear Magnetic Resonance Spectroscopy*; Jackman, L. M.; Cotton, F. A., Eds.; Academic Press: New York, 1975; pp 441–483.
- (20) Faller, J. W. In *Dynamic NMR Spectroscopy in Organometallic Chemistry, Comprehensive Organometallic Chemistry III*; Crabtree, R. H.; Mingos, D. M. P., Eds.; Elsevier: Oxford, 2006; pp 407–428.
- (21) (a) Cesarotti, E.; Grassi, M.; Prati, L.; Demartin, F. *J. Organomet. Chem.* **1989**, *370*, 407–419. (b) Cesarotti, E.; Grassi, M.; Prati, L.; Demartin, F. *J. Chem. Soc., Dalton Trans.* **1991**, 2073–2082.
- (22) (a) Fernandez-Galan, R.; Jalon, F. A.; Manzano, B. R.; Rodriguez de la Fuente, J.; Vreahami, M.; Jedlicka, B.; Weissensteiner, W.; Jögl, G. *Organometallics* **1997**, *16*, 3758–3768. (b) Montoya, V.; Pons, J.; Garcia-Anton, J.; Solans, X.; Font-Bardia, M.; Ros, J. *Organometallics* **2007**, *26*, 3183–3190.
- (23) Gogoll, A.; Ornebro, J.; Grennberg, H.; Bäckvall, J. E. *J. Am. Chem. Soc.* **1994**, *116*, 3631–3632.
- (24) Montoya, V.; Pons, J.; Garcia-Anton, J.; Solans, X.; Font-Bardia, M.; Ros, J. *Organometallics* **2007**, *26*, 3183–3190.
- (25) Chernyshova, E. S.; Goddard, R.; Pörschke, K. R. *Organometallics* **2007**, *26*, 3236–3251.
- (26) Filipuzzi, S.; Pregosin, P. S.; Albinati, A.; Rizzato, S. *Organometallics* **2008**, *27*, 437–444.
- (27) Peng, H.; Song, G.; Li, Y.; Li, X. *Inorg. Chem.* **2008**, *47*, 8031–8034.
- (28) (a) Pregosin, P. S.; Salzmänn, R. *Coord. Chem. Rev.* **1996**, *155*, 35–68. (b) Herrmann, J.; Pregosin, P. S.; Salzmänn, R.; Albinati, A. *Organometallics* **1995**, *14*, 3311–3318.
- (29) (a) Breutel, C.; Pregosin, P. S.; Salzmänn, R.; Togni, A. *J. Am. Chem. Soc.* **1994**, *116*, 4067–4068. (b) Pregosin, P. S.; Salzmänn, R.; Togni, A. *Organometallics* **1995**, *14*, 842–847.
- (30) (a) Wassenaar, J.; van Zutphen, S.; Mora, G.; Le Floch, P.; Siegler, M. A.; Spek, A. L.; Reek, J. N. H. *Organometallics* **2009**, *28*, 2724–2734. (b) Moreno, A.; Pregosin, P. S.; Fuentes, B.; Veiros, L. F.; Albinati, A.; Rizzato, S. *Organometallics* **2009**, *28*, 6489–6506. (c) Deng, W.; You, S.; Hou, X.; Dai, L.; Xia, W.; Sun, J. *J. Am. Chem. Soc.* **2001**, *123*, 6508–6519.
- (31) Faller, J. W.; Wilt, J. C. *Organometallics* **2005**, *24*, 5076–5083.
- (32) (a) Mandal, S. K.; Gowda, G. A. N.; Krishnamurthy, S. S.; Nethaji, M. *Dalton Trans.* **2003**, 1016–1027. (b) Camus, J. M.; Andrieu, J.; Richard, P.; Poli, R. *Eur. J. Inorg. Chem.* **2004**, 1081–1091.
- (33) Filipuzzi, S.; Pregosin, P. S.; Albinati, A.; Rizzato, S. *Organometallics* **2006**, *25*, 5955–5964.

- (34) Dastgir, S.; Coleman, K. S.; Cowley, A. R.; Green, M. L. H. *Organometallics* **2010**, *29*, 4858–4870.
- (35) Parr, R. G.; Yang, W. *Density Functional Theory of Atoms and Molecules*; Oxford University Press: New York, 1989.
- (36) (a) Wiberg, K. B. *Tetrahedron* **1968**, *24*, 1083. (b) Wiberg indices are electronic parameters related to the electron density between atoms. They can be obtained from a natural population analysis and provide an indication of the bond strength.
- (37) (a) Marion, N.; Navarro, O.; Mei, J.; Stevens, E. D.; Scott, N. M.; Nolan, S. P. *J. Am. Chem. Soc.* **2006**, *128*, 4101–4111. (b) Piechaczyk, O.; Doux, M.; Ricard, L.; Le Floch, P. *Organometallics* **2005**, *24*, 1204–1213.
- (38) Wolfe, J. P.; Buchwald, S. L. *Angew. Chem., Int. Ed.* **1999**, *38*, 2413–2416.
- (39) Perrin, D. D.; Armarego, W. L. F. *Purification of Laboratory Chemicals*, 3rd ed.; Pergamon: New York, 1988.
- (40) (a) Knebel, W. J.; Angelici, R. J. *Inorg. Chim. Acta* **1973**, *7*, 713–716. (b) Knebel, W. J.; Angelici, R. J. *Inorg. Chem.* **1974**, *13*, 632–637. (c) Ainscough, E. W.; Brodie, A. M.; Wong, S. T. *J. Chem. Soc., Dalton Trans.* **1977**, 915–920.
- (41) Öztopcu, Ö.; Puchberger, M.; Mereiter, K. A.; Kirchner, K. *Dalton Trans.* **2011**, *40*, 7008–7021.
- (42) Auburn, P. R.; Mackenzie, P. B.; Bosnich, B. *J. Am. Chem. Soc.* **1985**, *107*, 2033–2046.
- (43) Bruker programs: APEX2, version 2009.9-0; SAINT, version 7.68 A; SADABS, version 2008/1; SHELXTL, version 2008/4; Bruker AXS Inc.: Madison, WI, 2009.
- (44) Sheldrick, G. M. *Acta Crystallogr.* **2008**, *A64*, 112–122.
- (45) Frisch, M. J.; Trucks, G. W.; Schlegel, H. B.; Scuseria, G. E.; Robb, M. A.; Cheeseman, J. R.; Montgomery, J. A., Jr.; Vreven, T.; Kudin, K. N.; Burant, J. C.; Millam, J. M.; Iyengar, S. S.; Tomasi, J.; Barone, V.; Mennucci, B.; Cossi, M.; Scalmani, G.; Rega, N.; Petersson, G. A.; Nakatsuji, H.; Hada, M.; Ehara, M.; Toyota, K.; Fukuda, R.; Hasegawa, J.; Ishida, M.; Nakajima, T.; Honda, Y.; Kitao, O.; Nakai, H.; Klene, M.; Li, X.; Knox, J. E.; Hratchian, H. P.; Cross, J. B.; Adamo, C.; Jaramillo, J.; Gomperts, R.; Stratmann, R. E.; Yazyev, O.; Austin, A. J.; Cammi, R.; Pomelli, C.; Ochterski, J. W.; Ayala, P. Y.; Morokuma, K.; Voth, G. A.; Salvador, P.; Dannenberg, J. J.; Zakrzewski, V. G.; Dapprich, S.; Daniels, A. D.; Strain, M. C.; Farkas, O.; Malick, D. K.; Rabuck, A. D.; Raghavachari, K.; Foresman, J. B.; Ortiz, J. V.; Cui, Q.; Baboul, A. G.; Clifford, S.; Cioslowski, J.; Stefanov, B. B.; Liu, G.; Liashenko, A.; Piskorz, P.; Komaromi, I.; Martin, R. L.; Fox, D. J.; Keith, T.; Al-Laham, M. A.; Peng, C. Y.; Nanayakkara, A.; Challacombe, M.; Gill, P. M. W.; Johnson, B.; Chen, W.; Wong, M. W.; Gonzalez, C.; Pople, J. A. *Gaussian 03*, Revision C.02; Gaussian, Inc.: Wallingford, CT, 2004.
- (46) Hehre, W. J.; Radom, L.; Schleyer, P. v.R.; Pople, J. A. *Ab Initio Molecular Orbital Theory*; John Wiley & Sons: New York, 1986.
- (47) (a) Perdew, J. P.; Burke, K.; Ernzerhof, M. *Phys. Rev. Lett.* **1997**, *78*, 1396. (b) Perdew, J. P. *Phys. Rev. B* **1986**, *33*, 8822.
- (48) (a) Dunning, T. H., Jr.; Hay, P. J. *Modern Theoretical Chemistry*; Schaefer, H. F. III, Ed.; Plenum: New York, 1976; Vol. 3, p 1. (b) Hay, P. J.; Wadt, W. R. *J. Chem. Phys.* **1985**, *82*, 270. (c) Wadt, W. R.; Hay, P. J. *J. Chem. Phys.* **1985**, *82*, 284. (d) Hay, P. J.; Wadt, W. R. *J. Chem. Phys.* **1985**, *82*, 2299.
- (49) Ehlers, A. W.; Böhme, M.; Dapprich, S.; Gobbi, A.; Höllwarth, A.; Jonas, V.; Köhler, K. F.; Stegmann, R.; Veldkamp, A.; Frenking, G. *Chem. Phys. Lett.* **1993**, *208*, 111.
- (50) (a) Ditchfield, R.; Hehre, W. J.; Pople, J. A. *J. Chem. Phys.* **1971**, *54*, 724. (b) Hehre, W. J.; Ditchfield, R.; Pople, J. A. *J. Chem. Phys.* **1972**, *56*, 2257. (c) Hariharan, P. C.; Pople, J. A. *Mol. Phys.* **1974**, *27*, 209. (d) Gordon, M. S. *Chem. Phys. Lett.* **1980**, *76*, 163. (e) Hariharan, P. C.; Pople, J. A. *Theor. Chim. Acta* **1973**, *28*, 213.
- (51) (a) Peng, C.; Ayala, P. Y.; Schlegel, H. B.; Frisch, M. J. *J. Comput. Chem.* **1996**, *17*, 49. (b) Peng, C.; Schlegel, H. B. *Isr. J. Chem.* **1994**, *33*, 449.
- (52) (a) Carpenter, J. E.; Weinhold, F. *J. Mol. Struct. (THEOCHEM)* **1988**, *169*, 41. (b) Carpenter, J. E. Ph.D. thesis, University of Wisconsin, Madison WI, 1987. (c) Foster, J. P.; Weinhold, F. *J. Am. Chem. Soc.* **1980**, *102*, 7211. (d) Reed, A. E.; Weinhold, F. *J. Chem. Phys.* **1983**, *78*, 4066. (e) Reed, A. E.; Weinhold, F. *J. Chem. Phys.* **1983**, *78*, 1736. (f) Reed, A. E.; Weinstock, R. B.; Weinhold, F. *J. Chem. Phys.* **1985**, *83*, 735. (g) Reed, A. E.; Curtiss, L. A.; Weinhold, F. *Chem. Rev.* **1988**, *88*, 899. (h) Weinhold, F.; Carpenter, J. E. *The Structure of Small Molecules and Ions*; Plenum: New York, 1988; p 227.
- (53) (a) Haeusermann, U.; Dolg, M.; Stoll, H.; Preuss, H. *Mol. Phys.* **1993**, *78*, 1211. (b) Kuechle, W.; Dolg, M.; Stoll, H.; Preuss, H. *J. Chem. Phys.* **1994**, *100*, 7535. (c) Leininger, T.; Nicklass, A.; Stoll, H.; Dolg, M.; Schwerdtfeger, P. *J. Chem. Phys.* **1996**, *105*, 1052.
- (54) (a) McClean, A. D.; Chandler, G. S. *J. Chem. Phys.* **1980**, *72*, 5639. (b) Krishnan, R.; Binkley, J. S.; Seeger, R.; Pople, J. A. *J. Chem. Phys.* **1980**, *72*, 650. (c) Wachters, A. J. H. *J. Chem. Phys.* **1970**, *52*, 1033. (d) Hay, P. J. *J. Chem. Phys.* **1977**, *66*, 4377. (e) Raghavachari, K.; Trucks, G. W. *J. Chem. Phys.* **1989**, *91*, 1062. (f) Binning, R. C., Jr.; Curtiss, L. A. *J. Comput. Chem.* **1990**, *11*, 1206. (g) McGrath, M. P.; Radom, L. *J. Chem. Phys.* **1991**, *94*, 511. (h) Clark, T.; Chandrasekhar, J.; Spitznagel, G. W.; Schleyer, P. v. R. *J. Comput. Chem.* **1983**, *4*, 294. (i) Frisch, M. J.; Pople, J. A.; Binkley, J. S. *J. Chem. Phys.* **1984**, *80*, 3265.
- (55) (a) Cancès, M. T.; Mennucci, B.; Tomasi, J. *J. Chem. Phys.* **1997**, *107*, 3032. (b) Cossi, M.; Barone, V.; Mennucci, B.; Tomasi, J. *Chem. Phys. Lett.* **1998**, *286*, 253. (c) Mennucci, B.; Tomasi, J. *J. Chem. Phys.* **1997**, *106*, 5151.
- (56) (a) Tomasi, J.; Mennucci, B.; Cammi, R. *Chem. Rev.* **2005**, *105*, 2999. (b) Cossi, M.; Scalmani, G.; Rega, N.; Barone, V. *J. Chem. Phys.* **2002**, *117*, 43.